Electrical stresses on a selfsupporting metal-free optical fibre cable in high voltage networks

Berkers, A.G.W.M.

Award date:
1987

DEPARTMENT OF ELECTRICAL ENGINEERING

High Voltage Laboratory (EHO)

Electrical stresses on a selfsupporting metal-free optical fibre cable in high voltage networks.

EH.87.A.88.

A.G.W.M. Berkers

April, 1987.

Report of project for Ir. degree.

Supervisors:

dr.ir. J.M. Wetzer

prof.dr.ir. P.C.T. van der Laan

EINDHOVEN UNIVERSITY OF TECHNOLOGY

Abstract

Electricity companies need telecommunication for measurements and control. Today optical fibre systems are more and more used for this purpose. A possible way to install an optical communication link is to suspend a selfsupporting metal-free optical fibre cable in the high voltage overhead transmission and distribution lines. Electrical stress mechanisms give an important contribution to the ageing of the cable. Corona at the end of the suspension spiral and tracking are the two most important mechanisms. Calculations and measurements show that the choice of an optimal suspension position of the cable in the tower can prevent corona and considerably decrease the amount of tracking. The amount of tracking can also be decreased by a lower resistance of the cable sheath or by the application of a somewhat conductive layer underneath the sheath. The use of a strongly tracking resistant sheath material will decrease the damage to the cable surface caused by tracking discharges.

Contents

1. Introduction

Electricity companies need to know the present status (voltage, current, cosø) of their transmission and distribution lines at any moment. Also the status of the ambient air is important (temperature, wind velocity, etc.). Furthermore, telecommunication is required for remote controlled switches and, of course, audio and video signals. Until recently, information was transmitted by copper wires, carrier waves on phase lines, microwave systems and telephone lines. Because of the recent developments in optical fibre systems, these systems are now commercially available for the electricity supply industries.
Some important benefits of the use of optical fibre systems, compared to the wire systems mentioned above, are[4] the high obtainable bandwidth, low attenuation and the insensitivity to EMI (electromagnetic interference). Comparing optical fibre systems to microwave systems is more difficult because of the different legal limitations that are involved. Comparing the costs of telecommunication systems is outside the scope of this work, though important.
There are various methods to install an optical fibre cable in a high voltage network, e.g. fibres in the earthwire (or a phase conductor), fibre cable lashed around the earthwire (or a phase conductor) and metal-free selfsupporting cable. The last is more advantageous[1] for later-on installation on existing over-head (OH) lines. The first cable of this type was installed autumn 1982 at the "Rheinisch-Westfälischen Elektrizitätswerk AG" in a 110/220/380 kV line.[2]
Subject of this report are the electrical stress mechanisms that cause ageing of a metal-free, selfsupporting, aerial, optical fibre cable. First a literature study was performed which is reported in chapter 3. In order to quantify the stress mechanisms, calculations were made in chapter 4. Evaluation of the results of these calculations requires knowledge on material and system properties. Report on the measurements of these properties is given respectively in chapter 5 and 6. Discussion and conclusions are given respectively in chapter 7 and 8.

This study was performed on request of and in cooperation with "NKF Telecommunicatiekabels B.V.", which company also supplied the cable samples of the type shown in figure 1.1 and 1.2 [3].

Aerial optical fibre cable cross section:

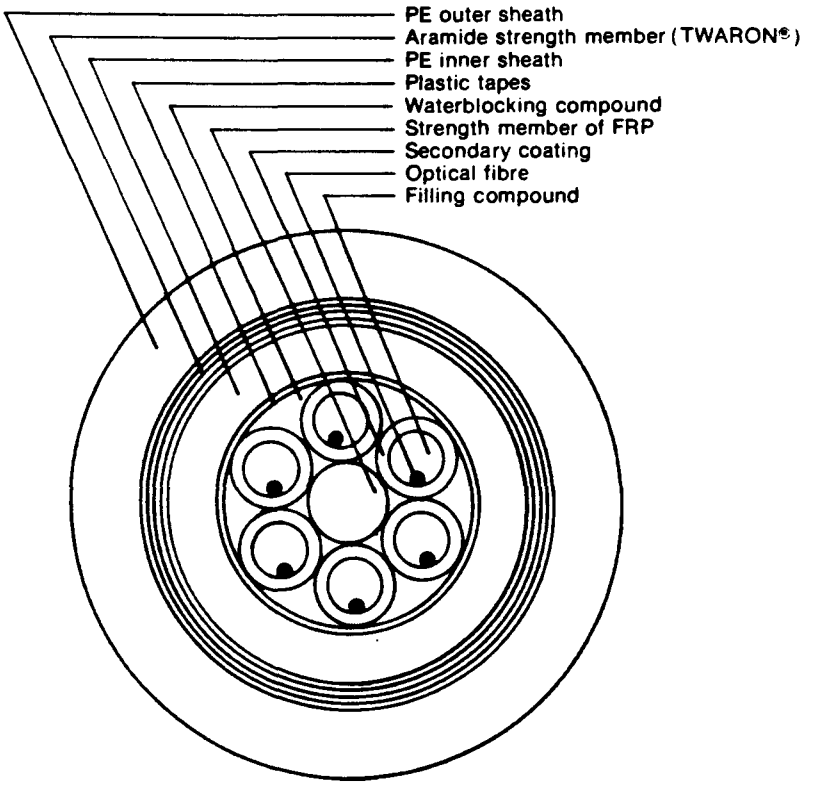

figure 1.1: NKF optical fibre cable.

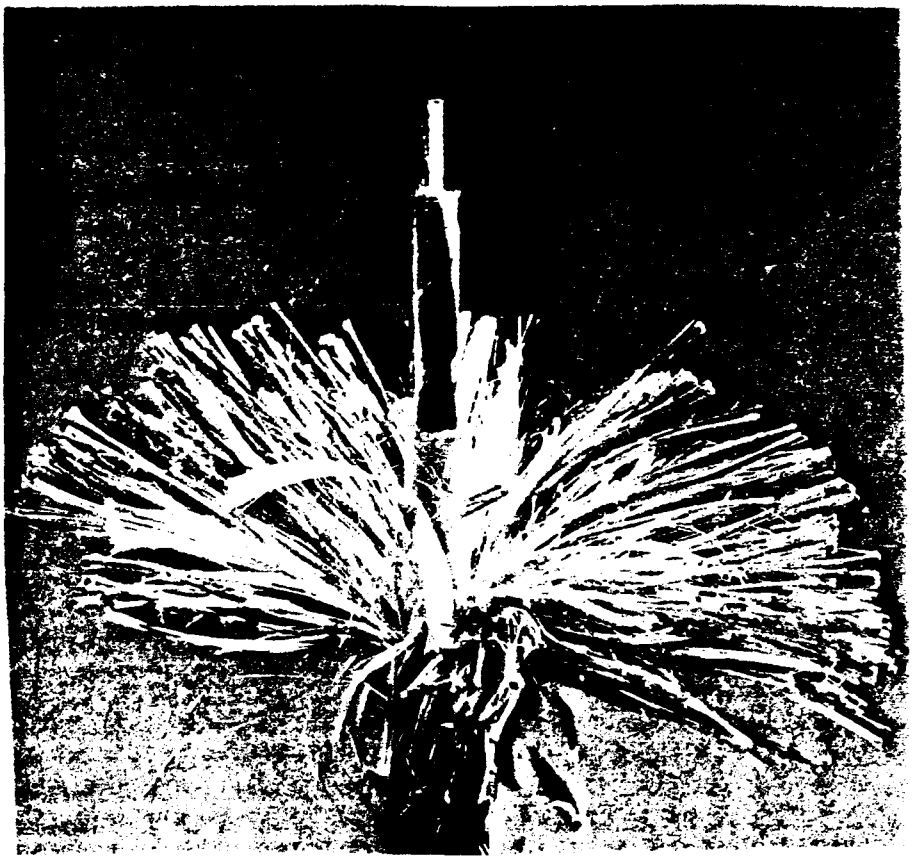

figure 1.2: NKF optical fibre cable.

2. Definitions

ageing: deterioration in time as a result of stresses.
arc: relatively stable electrical discharge carrying a high current.
arcing=scintillation: the (repetitive) ignition, extinction and movement of arcs. Arcing can result in tracks or erosion.
carbon black: high purity carbon powder.
dry arc resistance = corona resistance: a quantitative expression of the time required to make an arc of specified current penetrate into the nearby insulating surface.
electrical discharge: conductive path in a gas, bridging a gap between electrodes, carrying a small current.
corona[2]: often luminous and audible partial discharges in a non-uniform field.
flashover[1]: an electrical discharge at the surface of electrical insulation or in the surrounding medium, which may cause permanent damage to the insulation.
partial discharge: conductive path, bridging part of a gap. Though not carrying a conductive current, it may carry a significant capacitive current due to the small risetimes involved.
stress: all forces and other phenomena that may effect a specimens characteristics in a negative way.
surface conductivity[1]: the apparant DC conductance between two electrodes in contact with the surface of a specimen of insulating material related to the surface dimensions, when the current involved is limited to a thin film of moisture or other semi-conducting material on the surface of this specimen. (Some volume conductance is unavoidably included in actual measurements.)
surface resistivity: the reciproke of the surface conductivity.
track[1]: a more or less conducting path of localized deterioration on the surface of an insulating material.
tracking[1]: the process that produces tracks as a result of the action of electric discharges on or close to the insulation surface.
tracking resistance[1]: the quantitative expression of the voltage and time required to develop a track under specified conditions.

3. Ageing of optical fibre cable (literature study)

Equipment for high voltage networks is usually designed for 30 years life-time. Until now there is no such long service experience in the case of optical fibre cables.
The sheath of an aerial cable suffers from meteorological (uv radiation, water, wind, temperature, etc.), environmental (pollution accumulation) and mechanical (own weight, shot-gun damage, bird damage) influences, which cause surface degradation. Partial discharges on or near the surface enhance the ageing. The life-time of a cable depends on the combination of stresses on one hand and the construction of the cable and the choice of materials, on the other hand.
Because of the limited amount of literature related directly to the subject, (organic) outdoor HV insulators are studied also since they are subject to the same kind of stress.

3.1. Ageing mechanisms.

An important electrical stress mechanism is arcing along an insulator surface, because it can cause tracks or erosion and thus deteriorate the insulator surface. An essential condition for the occurrance of tracks is the presence of carbon On HV insulators this mechanism can cause flashover. Therefore the deterioration of an artificially aged insulator is often measured in terms of flashover voltage (f.o.v.)[2-9]. Arcing, or scintillation can start in two ways[31], which can occur simultaneously:

- A conductive film (water, possibly polluted) bridges an increasing part of the gap. The field along the remaining, dry, part increases until arcing is initiated (figure 3.1.1). Even though the distance is small, in the order of micrometers, the ignition voltage is relatively high; that is about 400 V, which is about the minimum breakdown voltage in Paschen's law.
- A relatively high leakage current may cause evaporation at locations where the current density is high or the conductivity is low (figure 3.1.2). This high current density will produce locally a lot of heat. Therefore a considerable number of charge carriers will be produced at the instant of disruption. The arc needs now a relatively small voltage to continu.

In both cases arcing may be extinguished when the gap increases by further evaporation.

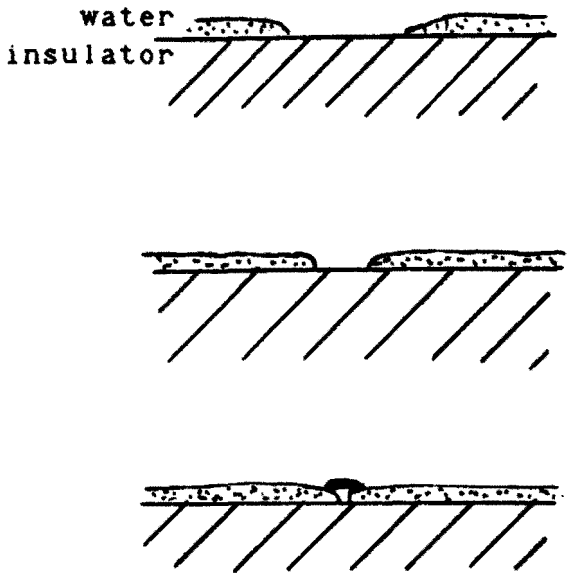

figure 3.1.1: Arc initiation from non conducting state.

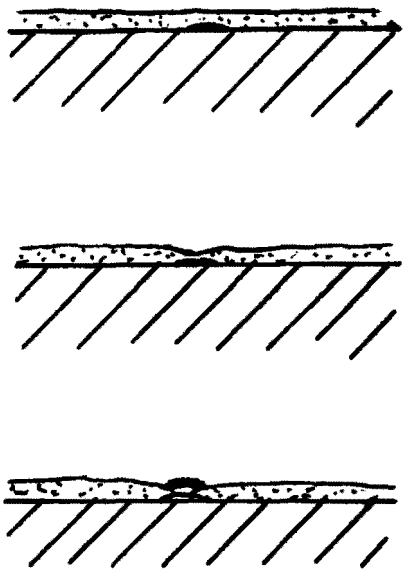

figure 3.1.2: Arc initiation from conducting state.

The literature, e.g. references [10,11,12], that reports on the research on the process that leads from arcing to flashover, is important for insulators, but not for cables, because the optical fibre cable doesn't bridge two electrodes.
The probability and intensity of arcing depend, in addition to the voltage, also on the properties of the conductive film that surrounds the insulator[10]. The conductive film consists of water with different soluble salts (most sulphates and chlorides[4]) and can vary in thickness from 0.1 to 600 μm[13]. The thickness of the layer depends on the surface characteristics of the insulator and on the properties of the salts that are present. The surface characteristics can be described by a set of parameters:

- water repellency[12] can be expressed in the angle between a drop of water and the technical clean surface (contact angle) (figure 3.1.3).
- apparant porosity[4] is expressed as the ratio of the volume of open pores of the specimen (freshly crushed fragments of insulator skirts) to its exterior volume.
- water absorption[4] is expressed as the ratio of the water absorbed to the weight of the dry specimen.

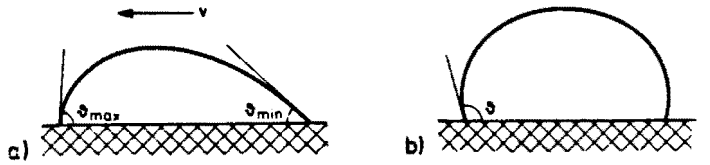

a: moving drop
b: drop in rest

figure 3.1.3: water repellency

The water repellency of an insulator surface decreases during ageing[4,13], because of corrosion and chemical attack caused by weathering conditions (pollution and irradiation[9]). Chemical nature and physical form of pollutant strongly affect the rate of detoriation[4]. The roughness of the insulator surface also has an influence on arcing. Lewis et al.[34] found that a rough insulator surface exhibited considerable tracking resistance compared to a smooth surface. This can be understood by looking at it as an increase in creepage distance.
There are also some electrical properties to characterize the surface of an insulator (defined in chapter 2):
- surface resistivity (IEC 93 [32])
- tracking resistance (IEC 112, 587 [21, 33])
- dry arc resistance (corona resistance) (ASTM D495 [19])

In non-uniform electric field configurations various manifestations of luminous and audible discharges are observed long before the complete breakdown occurs[35]. These discharges may be transient or steady state and are known as "corona". The phenomenon is of particular importance in HV engineering where non-uniform fields are unavoidable. It is responsible for power loss from HV transmission lines and often leads to deterioration of insulation by the combined action of the discharge ions bombarding the surface and the actions of chemical compounds that are formed by the discharge. The electric field strenght, at the surface of the conductor in air, required to produce a noticeable AC corona in air is about 25 - 30 kV/cm.

3.2. Optical cables in HV OH lines

In literature, 3 manufacterers of metal-free selfsupporting optical fibre cables (for OH lines) were found:

- NKF Telecommunicationcables (devision of NKF KABEL B.V.)[14]
- F&G (Felten & Guillaume) Telecommunicationcables and -systems (devision of Philips Kommunikations Industrie A.G.)[1]
- Standard Electric Lorenz AG [15]

All of them use PE (polyethylene) for the outer sheath of the cable. Recently NKF switched from LDPE (Low Density PE)

to HDPE (High Density PE)[16], because of the better transference of pulling force and the smaller sensibility to corona, see paragraph 3.3.1.
The importance of the HV fields to the ageing of the cable is described by Haag[17]. Because of the electrical properties of the sheath, the surface of the cable in the electrical field of the phase conductor gets charged by capacitive coupling (figure 3.2.1). The capacitances shown in the figure depend on the geometry of the optical cable, HV lines and earth.

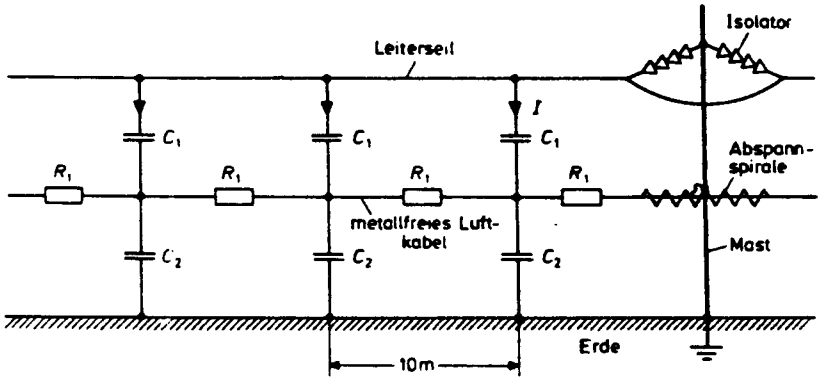

Modell für die Berechnung der kapazitiven Aufladung und Entladungsströme für metallfreie Luftkabel auf Freileitungsgestängen

figure 3. 2. 1.

The capacitance from the cable to earth is not constant over the whole lenght of the cable because of the influence of the grounded tower and the sag of the cable. This influence is not shown in figure 3.2.1. Since the surface resistance is high ($2 \cdot 10^8$ Ω/m - 10^{14} Ω/m)[17], the induced charge cannot flow away. At each tower the cable is grounded. Near the clamps at the tower high electric fields can occur. When the cable gets polluted and wet, the problems described in paragraph 3 (arcing, tracking) will occur. The capacitively induced voltage is considered[17] not important for 20 KV lines, in 110 KV lines no problems are expected, whereas it is the determining factor, for the life-time of the cable, in 220 KV and especially 380 KV lines.
In ref. [1] equipotential lines and electric field were determined graphically for a cable in a 110 KV OH line (see figure 3.2.2 and 3.2.3).

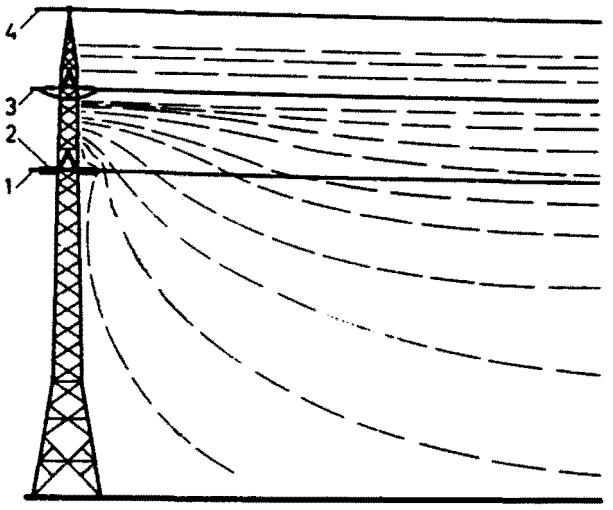

electric equipotential lines near the pole

1 non metallic optical fibre cable
2 metal dead ends
3 phase conductor
4 earth conductor

figure 3. 2. 2.

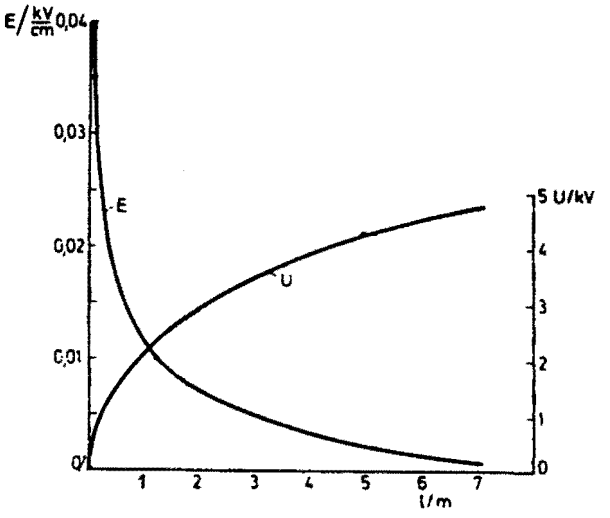

Induced voltage and electric force along the optical fibre cable beginning at the earthed dead-end (x=0)

figure 3. 2. 3.

Bartlett et al.[36] state that the main problem area for selfsupporting cables at the higher transmission voltages is degradation caused by the effect of the electric field on a cable sheath polluted by prevailing climatic conditions. It seems unlikely that this can be prevented by insulated support clamps[36]. The U.K. approach[36] to prevent the electrical degradation of the cable sheath, which at present limits the use of metal-free selfsupporting cables to voltages below about 110 kV, is to study sheath materials rather than to attempt to modify the cable or fittings near towers. Two approaches, of producing non-tracking and partially conducting sheaths, are being investigated.
Looking for remedies against tracking, engineers of Siemens[37] find a solution by providing the cable with a longitudinal resistance of 10^7 to 10^9 Ω/m and a jacket relatively insensitive to tracking and corona. Because of the lowered resistance, areas of high electrical stress between the borders of adjacent moist areas are then more or less electrically bridged thereby reducing tracking. Special outer jackets with a high content of aluminum hydroxide have[37] the suitable combination of the required physical properties. In addition to Barlett et al. the engineers of Siemens[37] also reject the method of insulated suspension.

A corona discharge close to the optical fibre cable can

cause deterioration as described in paragraph 3.1. Figure 3.2.4 shows the end of the Al/St (Aluminum/Steel) spiral that is often used to suspend the cable. Figure 3.2.5 shows the suspension spirals used for the NKF cable. Sharp edges at the end of the spiral might enhance the electric field strength above the corona onset level.

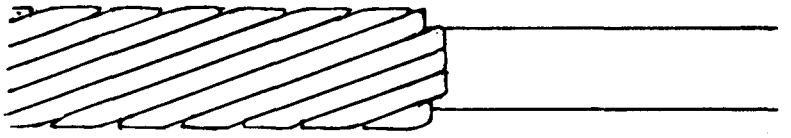

figure 3.2.4: End of spiral for cable suspension.

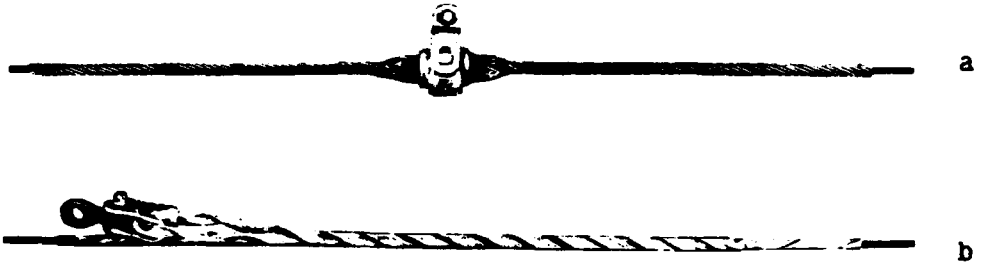

figure 3.2.5: Suspension spirals (a: suspension, b: tension) for NKF cable.

Furthermore[37] protruding irregularities on a possibly conducting cable surface can also cause radial discharges (corona), which erode and degrade the surface of the cable sheath.

Another electrical phenomenon that can damage the cable is caused by the possible soaking of the strenght member (aramide or FRP) when the outer sheath is damaged. The strength member of the NKF cable, aramide, has filaments of 12 µm with holes in between of 8 µm[16]. If these holes are filled with water, the resistance decreases. A problem occurs when the heat generated inside, by the resulting current, cannot flow away, or when the conductive area suddenly ends.

3.3. Material properties of polyethylene.

3.3.1. Arcing resistance

The dry arc resistance of a material can be determined by using the standard test procedures ASTM D495 or DIN 53 484. Mark[18] gives values for natural PE using the ASTM D495[19] method. In this test the arc resistance is described as the total elapsed time of operation until failure. Failure occurs when the arc, of specified current pattern, disappears into the tested material.

LDPE 135 - 160 s
MDPE 200 - 235 s
HDPE ---

3.3.2. Tracking and erosion resistance

To determine the tracking and erosion resistance different tests are used:

ASTM D2132
IEC 112
ASTM D2303

Parr and Scarisbrick[20] compared the IEC 112[21] with the ASTM D2132 test. The results are listed below.

	IEC 112(1959)		ASTM D2132(1962)	
	comparative tracking index	erosion index	failure mechanism	life
	V	V	-	h
LDPE	> 500	>750	erosion	60.0
LDPE + 2 % carbon black	> 500	---	tracking	0.9

The indices given by the IEC 112 test are the voltages at which failure (I > 0.5 A for 2 s) occurs before the 50 drops of test solution have fallen on the test surface. For the ASTM D2132 test the test specimen are artificially contaminated and placed in a specified fog. The time after applying 1500 V is measured until failure (I > 2 A). Parr and Scarisbrick concluded that the ASTM D2132[22] method is more adequate than the IEC 112 method.

Clabburn et al.[23] used the ASTM D2303[24] test to determine the influences of additives to the tracking behaviour of PE, see table 3.3.2.1. This tracking behaviour is expressed in the "initial tracking voltage" (ITV), which is determined in the test at a specified rate of contamination application.

Exposing PE to outdoor environment can also cause loss of tracking resistance, see also paragraph 3.3.6.

Absorber	ITV in KV
None	3.0
1% Carbon Black	2.0
2% Carbon Black	1.5
1% Fe_2O_3	2.75
1% Zn O	2.25
0.5% Uvinol 410 (substituted benzophenone)	2.5
0.5% Tinuvin P(substituted benzotriazole)	2.75

Trade Name	Antioxidant Type	ITV in KV
None	None	3.0
Agerite Resin D	Polymerised dihydro quinoline	2.5
Irganox 858	High molecular weight hindered phenol	3.0
Nonox WSL	Medium molecular weight hindered phenol.	2.0
Akroflex CD	Substituted diphenyl-amines	2.25
2246	Low molecular weight hindered phenol	2.75

table 3. 3. 2. 1: Effects of additives on ITV of PE.

3.3.3. Water repellency = Hydrophobocity

The water repellency of a material can be expressed in the contact angle between a water-drop and the surface.
McNicoll et al.[25] measured the contact angle between a water-drop and a PE surface:

- molded 94. 3
- cut by microtome 103. 5

When the PE suface is aged the contact angle becomes slowly smaller.

3.3.4. Surface resistance

The surface resistivity of PE depends strongly on the relative humidity (RH) of the surrounding air. Field[26] found that the surface resistivity decreases steadily to its equilibrium value, which is reached in about 100 minutes. Figure 3.3.4.1 shows the surface resistivity of PE as a function of RH. The resistivity at 100 % RH is $1.3 \cdot 10^9$ Ω. Licari[27] measured the surface resistivity of PE at 96 % RH:

fingerprint contaminated $5 \cdot 10^7$ Ω
freshly shaved surface $2.2 \cdot 10^{11}$ Ω

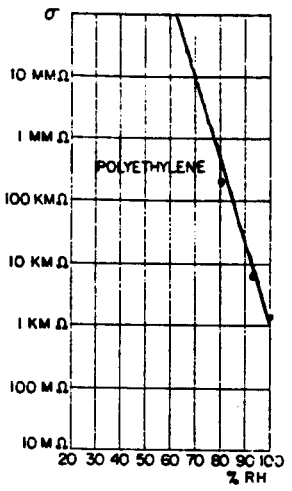

figure 3. 3. 4. 1: Surface resistivity of PE
(1 KMΩ = $10^3 \cdot 10^6$ Ω, etc.).

3.3.5. Water absorption

Several figures of water absorption in (natural) PE are found in literature (weight percentages):

[27]: in 24 h < 0. 01 %
[28]: in 30 days 0. 095 %
[29]: in 24 h, 1/8 inch thick:
LDPE < 0. 015 %
MDPE < 0. 01 %
HDPE < 0. 01 %

No comments are given on these figures.

3.3.6. Outdoor behaviour

Clabburn et al.[23] described the adverse effects on PE properties because of long term outdoor exposure. The contributing factors to these adverse effects are:

1. weather: - UV component of sunlight
   - atmospheric oxygen
   - moisture: rain, dew, etc.
2. pollution: - natural: sand, dust, salt, etc.
   - industrial: ash, gaseous wastes, etc.
3. thermal effects
4. mechanical effects

ad 1: UV light can break several different types of chemical bonds and thus cause chain scission in a polymer. Scission results in degradation of the polymer which may be recognized as loss of both mechanical and electrical properties such as strength, elongation, track resistance and the like. Free radicals are created also by UV light. In the presence of oxygen the formation of free radicals can lead to an auto-catalytic reaction by the generation of several further types of radicals i.e. a chain reaction of degrading ra-

dicals is initiated. Moisture can enhance this effect. An other effect of moisture is that the freezing of water in surface imperfections can cause cracks. The tendency towards oxidation can be largely prevented[18] by the incorporation of antioxidants into the polymer. Gilroy[30] found that the use of carbon black of over 1 % and of particle size of less than 35 μm has been found to be adequate to protect PE for over 38 years outdoor exposure.

ad 2: The main kinds of pollution that attack the polymer are: ozone and oxides of sulphur and nitrogen. The reaction of PE with ozone can proceed very rapidly at 60 C with gross chain scission. In the presence of UV light and sulphur dioxide PE gets crosslinked. Exposure to nitrogen dioxide results in incorporation of nitro groups into the backbone. This can cause a decrease of tracking resistance as shown in table 3.3.6.1.

Polymer	ITV, in KV
Polyethylene	3.0
Nitrated Polyethylene I	2.75
Nitrated Polyethylene II	2.25

Nitrated polyethylene I contained one nitro group per 430 carbon atoms
Nitrated polyethylene II contained one nitro group per 220 carbon atoms

table 3.3.6.1: Nitration of PE.

ad 3 and 4: High, low and suddenly changing temperatures can be expected. Problems can arise from the fact that different components of the cable have different coefficients of linear expansion, for example:

PE $2.5 \cdot 10^{-4}\ K^{-1}$
aramide $-2 \cdot 10^{-6}\ K^{-1}$

The consequence is that stresses will be present between PE and aramid. The stresses and strains may open and close micro cracks on the surface of the polymer. Moisture and solid pollutants become trapped in surface cracks. The trapped matter enhances tracking. These effects will clearly be accelerated by additional stresses resulting from wind, snow and ice loadings.

4. Model calculations

All computer calculations reported of in this chapter were performed on the B7900 system of the Technical University Eindhoven in the programming language Algol 60. The text of the "POTCALC" program (paragraph 4.1) is given in Appendix B.

4.1. Potential distribution perpendicular to the HV lines

4.1.1. Calculation method

For line-charges it is possible to calculate analytically the electric field. If the diameters of the conductors are small compared to the distances involved, then each conductor can be represented by one line charge.
The three phase sinusoidal system is represented by complex voltages as shown in figure 4.1.1.1. If U is the systems phase-phase voltage, then

$$V_R = \sqrt{3}U/3$$
$$V_S = -\sqrt{3}U/6 - jU/2$$
$$V_T = -\sqrt{3}U/6 + jU/2$$

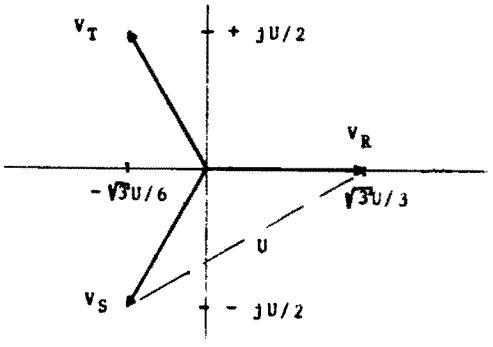

figure 4.1.1.1: Three phase sinusoidal system.

In the following, calculations are made using the effective voltages and the method of reference [1].

V_i (i = 1, 2, ... n) are the known voltages of the conductors

$$[V] = [VR] + j[VI] \qquad [Q] = [QR] + j[QI]$$

$$[QR] = [P]^{-1}[VR] \qquad [QI] = [P]^{-1}[VI]$$

and Q_i are the line charges calculated out of the voltages.
The elements of the matrix P are:

$$P_{ii} = -\frac{1}{2\pi\epsilon} \ln\left[\frac{d_i}{4y_i}\right]$$

$$P_{ij} = -\frac{1}{4\pi\epsilon} \ln\left[\frac{(x_i-x_j)^2+(y_i-y_j)^2}{(x_i-x_j)^2+(y_i+y_j)^2}\right]$$

where

y_i (m) height of conductor i above ground
d_i (m) diameter of conductor i
$(x_i, y_i), (x_j, y_j)$ (m) are the coordinates of the conductors i and j
and $y > 0$

It is convenient to consider a bundle of conductors as one single conductor having an equivalent diameter given by[1, 2]

$$d_{eq} = D\left[\frac{md}{D}\right]^{1/m}$$

where D is the bundle diameter, m is the number of subconductors, and d is the diameter of the subconductors.

The voltage in a point (x, y), somewhere in the conductor field can be derived from the superposition of the contributions of the individual conductors:

$$V(x, y) = \sum_{i=1}^{n} -\frac{Q_i}{4\pi\epsilon} \ln\left[\frac{(x_i-x)^2+(y_i-y)^2}{(x_i-x)^2+(y_i+y)^2}\right]$$

In the same way the electric field strength is calculated

$$E_x = \sum_{i=1}^{n} \frac{Q_i}{2\pi\epsilon}\left[\frac{x - x_i}{(x-x_i)^2+(y-y_i)^2} - \frac{x - x_i}{(x-x_i)^2+(y+y_i)^2}\right]$$

$$E_y = \sum_{i=1}^{n} \frac{Q_i}{2\pi\epsilon}\left[\frac{y - y_i}{(x-x_i)^2+(y-y_i)^2} - \frac{y + y_i}{(x-x_i)^2+(y+y_i)^2}\right]$$

The complete set of capacitances, C_{ij}, of the system is:

$C_{ii} = \sum_{j=1}^{n} K_{ij}$ capacitance between conductor i and earth

$C_{ij} = C_{ji} = -K_{ij}$ capacitance between conductors i and j

$[K] = [P]^{-1}$

4.1.2. Calculations on practical towers

Equipotential-lines were calculated for two PNEM (Noord Brabant Electricity Company) towers (one for 150 kV and one for 380 kV) and one (380 kV) EZH (South-Holland Electricity Company) tower. Results are shown in figures 4.1.2.1 to 4.1.2.3. For the EZH-tower there are three different phase distributions in use. They all give the same potential distributions.

Conductor diameters were calculated from the cross-section areas with

$$d = 2F\sqrt{(A/\pi)} \qquad \text{where} \qquad F = 1.15$$

The factor F was introduced because a phase or ground conductor is composed of twisted steel and aluminum wires. F was obtained by relating calculated diameters with real diameters given in a list of German standard conductors[4]. The standard deviation in F is (N = 8) 0.007.

The figures 4.1.2.1 to 4.1.2.3 show the situations in the middle between two towers, so the sag (different for phase

conductors and earth wires) is taken into account.
When an optical fibre cable with a slightly conducting sheath is suspended between the wires, the capacitances between cable and phase conductors, and between cable and ground will result in a cable potential which depends on the values of the capacitances. A typical set of capacitances is given in table 4.1.2.1. It is assumed that the sag of the cable is the same as the sag of the phase wires.

		capacitance (pF/m)	
		sag	no sag
phase-cable:	RC	2.09	2.14
	SC	1.89	1.94
	TC	1.84	1.88
cable-ground		1.48	1.34

table 4.1.2.1: Capacitances in tower 170 (cable in position (x = -8.53, y = 33.3), see figure 4.1.2.2).

The maximum radial electric field strength at the suspension spirals is calculated near the tower (no sag), without taking the influence of the tower into account. At the spiral-end this field strength will be enhanced. The enhancement factor can be determined in the measurements by calculating the electric field strength at the discharge onset voltage, and relating this value to the electric field strength needed for (corona) discharges, i.e. about 30 kV/cm.

Figure 4.2.1.1 shows a type of tower in which 8.5 km of optical fibre cable is suspended. The cable is suspended in position (0,12.75) which results in a potential of 15.6 kV. From the figure it can be seen that (±8.5,12.9) is a better position to suspend the cable because the potential there is 1.51 kV. The maximum radial electric field strength at suspension spiral is 1.57 kV/cm in (0,12.75).

Figure 4.1.2.2 shows a clear minimum in the potential distribution. This minimum is located in position (-8.53,33.3) and has a potential of 7.03 kV. The maximum radial electric field strenght at the suspension spiral in this position is 0.89 kV/cm. This configuration, see also table 4.1.2.1, is used for the calculations in paragraph 4.2.

In the tower shown in figure 4.1.2.3 the suspension of an optical fibre cable is planned. There were three possible suspension positions, (0,28.35) and (±4.08,49.4). From the

figure it is clear for the reason of cable potential, position (0,28.35) with a potential of 3.43 KV has to be chosen. The maximum radial electric field strength at the suspension spiral in this position is 0.27 KV/cm.

tower type = 163PNEM112.540-1
d_{eq}(phase) = 3.61 cm
d(ground) = 1.17 cm
U = 150 kV

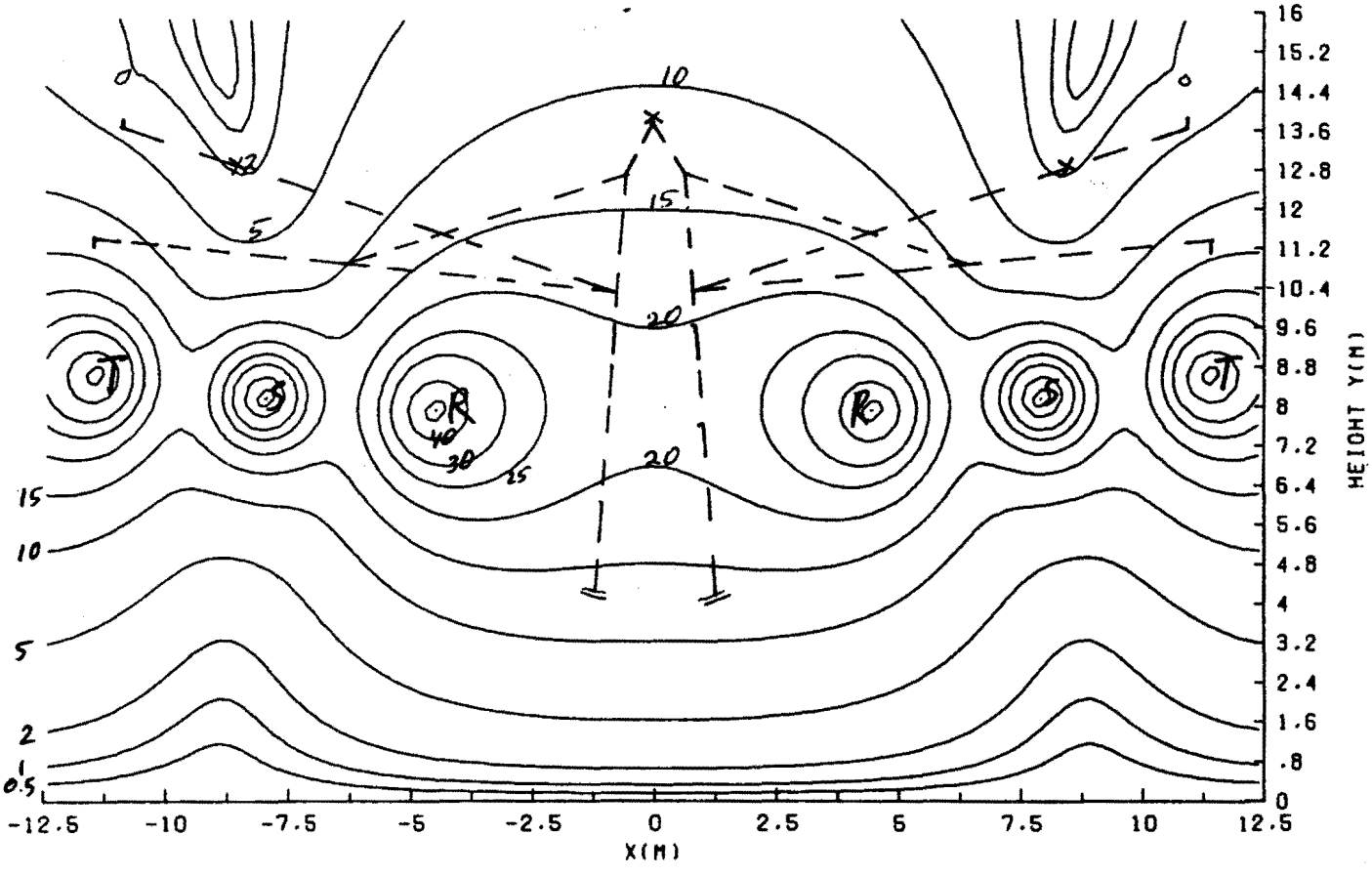

figure 4.1.2.1.

tower type = 170PNEM43.686
d_{eq}(phase) = 26.15 cm
d(ground) = 2.05 cm
U = 380 kV

EQUIPOTENTIAL LINES FOR V= 0.5.1.2.5.10.15.20.25.30.40.60.80 % OF 219.4 KV(PH-GR)

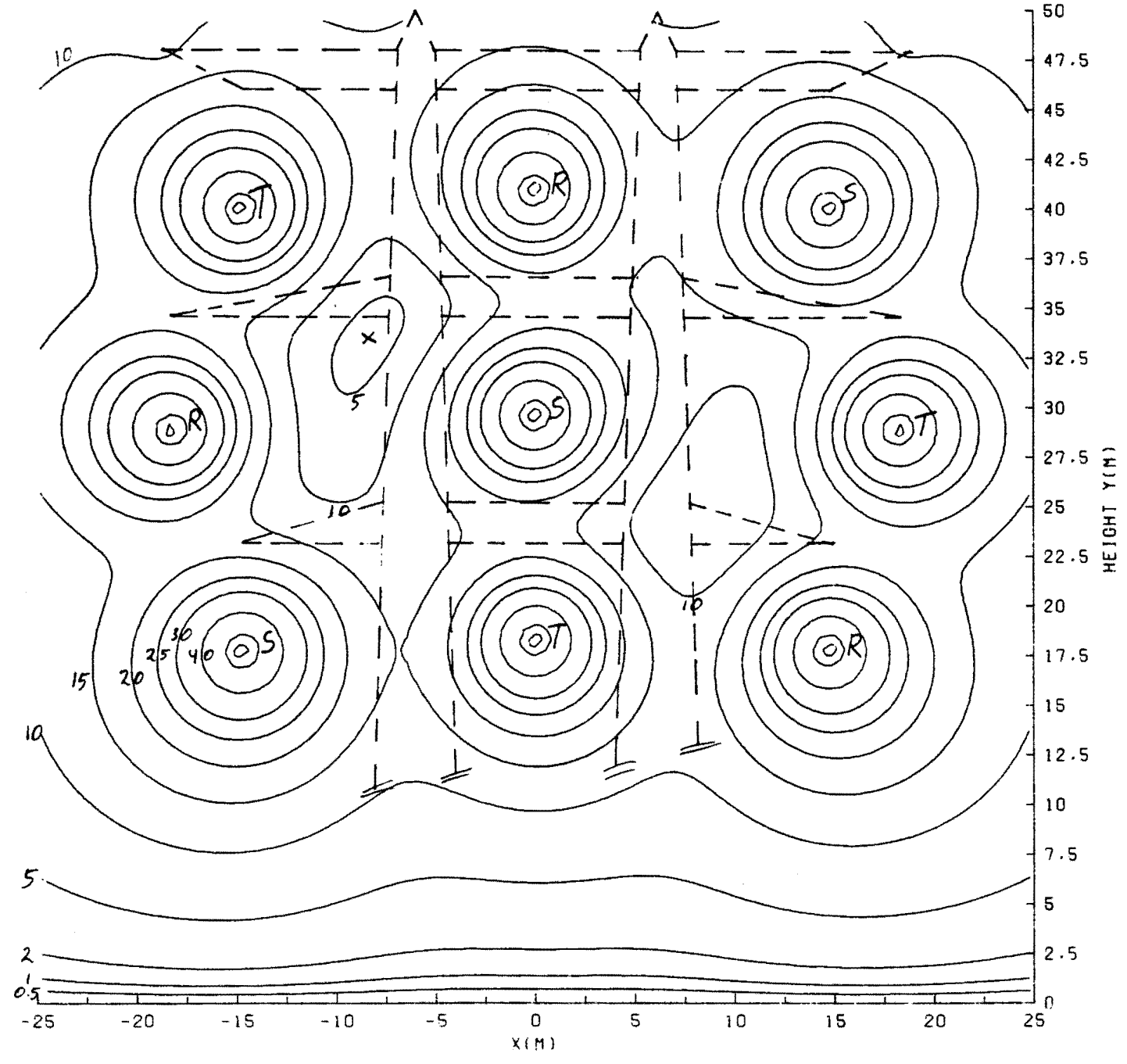

figure 4.1.2.2.

tower type = EZH/FD/432
d_{eq}(phase) = 39.3 cm
d(ground) = 2.18 cm
U = 380 kV

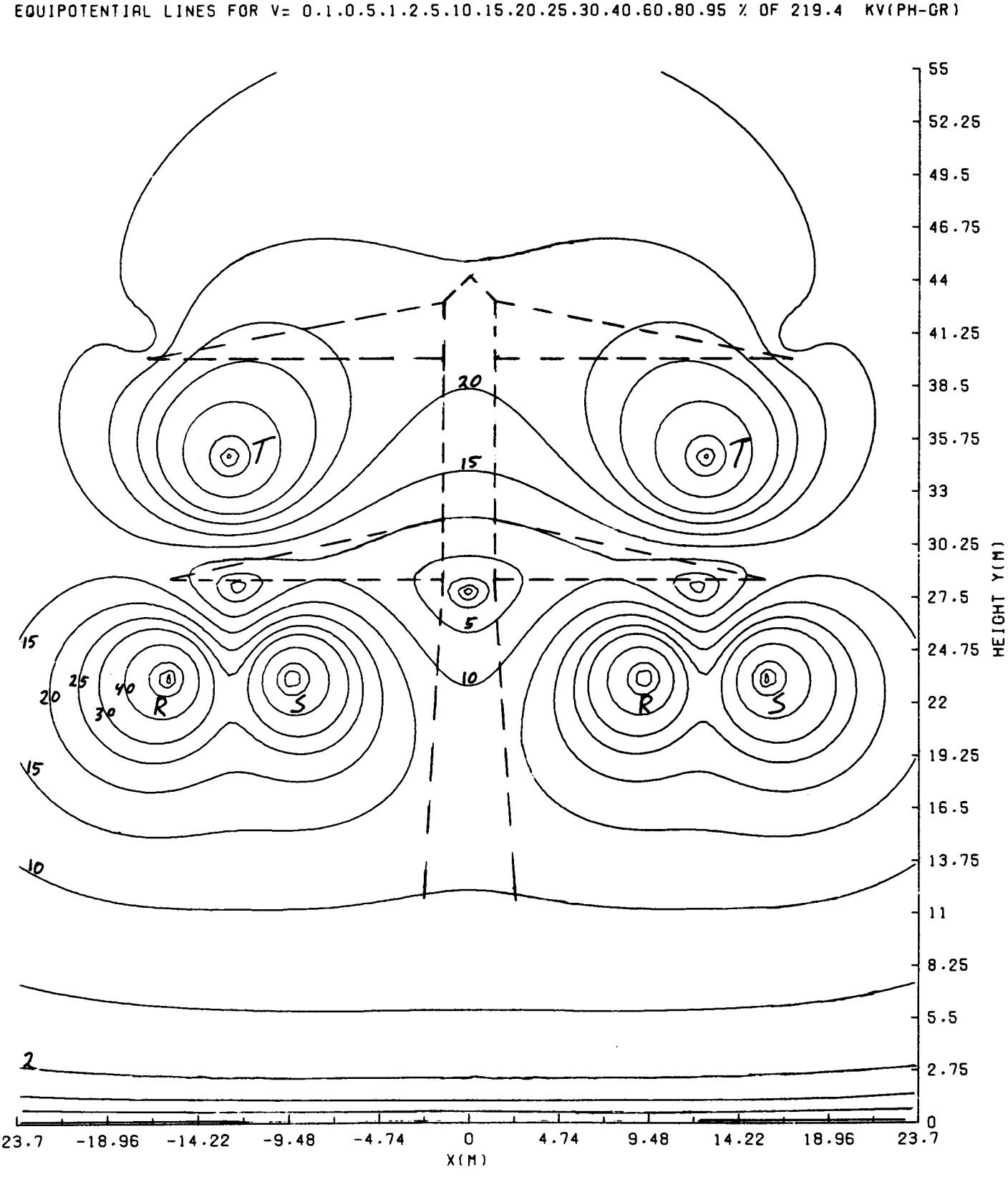

figure 4.1.2.3.

4.2. Voltage distribution along the optical fibre cable.

4.2.1. Calculation method.

The optical fibre cable is suspended parallel to the phase conductors. In the calculations these phase conductors are considered to be "ideal" voltage sources, i.e. with negligible output impedance. The system of m phase conductors (figure 4.2.1.1) can be replaced by one Thevenin equivalent voltage source, calculated as follows (c in F/m)

$$c_s = c_1 + c_2 + c_3 + \ldots . c_m$$
$$V_s = (c_1V_1 + c_2V_2 + \ldots . c_mV_m)/c_s$$

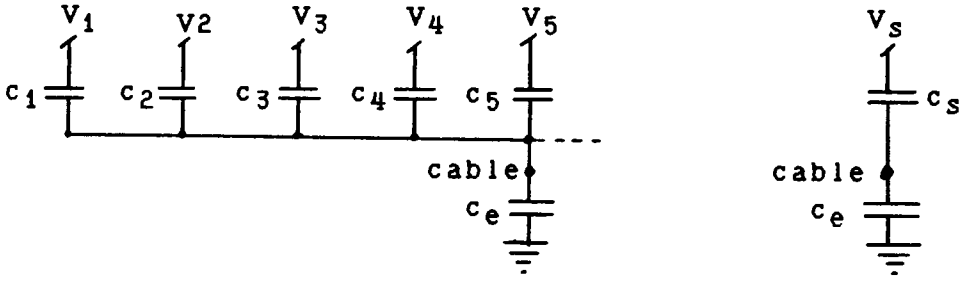

figure 4.2.1.1.

A small piece, Δx, of the cable can be replaced by

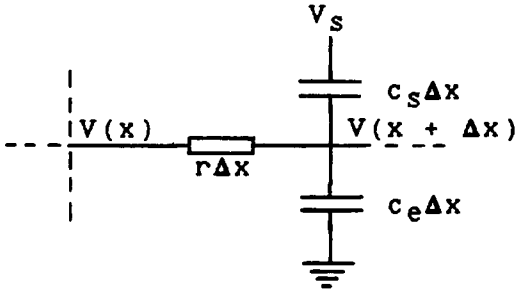

figure 4.2.1.2.

where r[Ω/m] and c_s, c_e[F/m]. This leads to the following differential equations (Δx → 0)

$$\frac{\partial V}{\partial x} = -rI$$

$$\frac{\partial I}{\partial x} = c_s\frac{\partial V_s}{\partial t} - (c_e + c_s)\frac{\partial V}{\partial t}$$

$$\frac{\partial^2 V}{\partial x^2} = -rc_s\frac{\partial V_s}{\partial t} + r(c_e + c_s)\frac{\partial V}{\partial t}$$

When the excitation is sinusoidal and c_s, c_e and r are constant then the differential equations become

$$\frac{dV}{dx} = -rI$$

$$\frac{dI}{dx} = j\omega c_s V_s - j\omega(c_e + c_s)V$$

$$\frac{d^2V}{dx^2} - j\omega r(c_e + c_s)V = -j\omega r c_s V_s$$

and have a solution

$$V(x) = Ae^{\gamma x} + Be^{-\gamma x} + V_p$$
$$I(x) = -AZ^{-1}e^{\gamma x} + BZ^{-1}e^{-\gamma x}$$
$$E(x) = rI(x)$$

where

$$V_p = \frac{c_s V_s}{c_s + c_e}$$

$$Z = \sqrt{\left[\frac{r}{j\omega(c_s+c_e)}\right]}$$

$$\gamma = \sqrt{[j\omega r(c_s+c_e)]}$$

This model is similar to the transmission line model of Thomson (Lord Kelvin).
The cable is grounded at each suspension tower and the system is assumed to be symmetric around x=L (figure 4.2.1.3), so

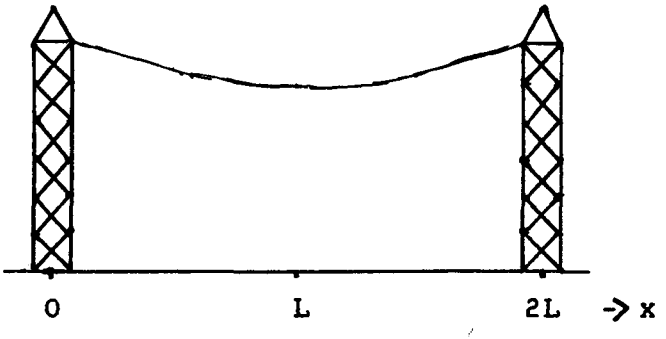

figure 4.2.1.3.

$$V(0) = 0$$
$$V(2L) = 0$$
$$I(L) = 0$$

Because of the symmetry, calculations are performed for $0 < x < L$.
So far r and c_e were assumed independent on x. In order to extend the model to x-dependent impedances the cable-half is divided into n pieces of variable length, with resistance and capacitance values $r_i[\Omega/m]$ and $c_{ei}[F/m]$:

$x_0=0$, $x_n=L$

$0 < x < x_1$	γ_1, Z_1, V_{p1},	A_1, B_1
$x_{i-1} < x < x_i$	γ_i, Z_i, V_{pi},	A_i, B_i
$x_{n-1} < x < L$	γ_n, Z_n, V_{pn},	A_n, B_n

Now for each section the solution is represented by constants A_i, B_i, V_{pi}, Z_i, γ_i, where P_i, Z_i and γ_i follow directly from the impedance values and the source voltage. A_i and B_i have to be calculated from the boundary conditions of each section:

$$V_i(x_i) = V_{i+1}(x_i)$$
$$I_i(x_i) = I_{i+1}(x_i)$$

or

$$A_i e^{\gamma_i x_i} + B_i e^{-\gamma_i x_i} + V_{pi} = A_{i+1} e^{\gamma_{i+1} x_i} + B_{i+1} e^{-\gamma_{i+1} x_i} + V_{pi+1}$$

$$\frac{A_i}{Z_i} e^{\gamma_i x_i} + \frac{B_i}{Z_i} e^{-\gamma_i x_i} = \frac{A_{i+1}}{Z_{i+1}} e^{\gamma_{i+1} x_i} + \frac{B_{i+1}}{Z_{i+1}} e^{-\gamma_{i+1} x_i}$$

$$\text{for } i = 1 \ldots\ldots n-1$$

and

$$V(0) = 0$$
$$I(L) = 0$$

This results in a set of 2n equations for the determination of $A_1 \ldots A_n$ and $B_1 \ldots B_n$.

The grounded tower influences the electric field nearby and changes the cable-earth capacitance. The cable is suspended to the tower with a 2 m Al/St spiral. So the point were the cable is grounded is about 2 m away from the tower. With help of reference [6] it is possible to calculate the capacitance between an infinite surface and a rod of length l

perpendicular to that surface. The distance between rod and surface is assumed to be negligibly small. To calculate the capacitance per unit of length, the derivate to the length l is taken. The result is

$$\frac{dC}{dl} = \frac{2\pi\epsilon\left[\ln\frac{2l}{d\sqrt{3}} - 1\right]}{\left[\ln\frac{2l}{d\sqrt{3}}\right]^2}$$

This capacitance gives the absolute maximum of the tower influence. For practical situations, i.e. a frame-work tower, the real influence of the tower is approximated to be half of this limit value. Then the total capacitance from cable to earth is for x=0 at 2 m from the tower

$$x = 0 \qquad c'_e \approx \frac{1}{2}\cdot\frac{dC}{dl}(l=2) + c_e = 4.5 \text{ pF/m} + c_e$$

4.2.2. Results.

In paragraph 4.1 a preferable place is given for suspending the optical fibre cable in PNEM tower 170,43.686 (380 kV). The cable-phase and the cable-ground capacitances of this system are:

$c_{RC} = 2.09$ pF/m
$c_{SC} = 1.89$ pF/m
$c_{TC} = 1.84$ pF/m
$c_e = 1.48$ pF/m

which results in

$V_s = 8.62 + j(-1.86)$ kV
$c_s = 5.82$ pF/m

These capacitances result in a cable potential of V_p = 7.03 kV when there is no current flowing on the cable. Knowing the span-length to be 400 m (L = 200 m), calculations can be made for different values of r. Three typical shapes of the voltage distribution can be distinguished,

which are also valid for other systems. They are shown in figure 4.2.2.1.

1. Re(yL) << 2.15
2. Re(yL) = 2.15
3. Re(yL) >> 2.15

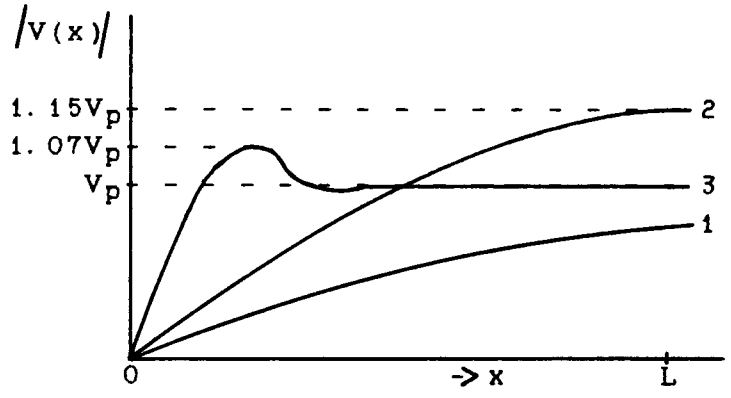

figure 4.2.2.1.

Figures 4.2.2.2 to 4.2.2.3 show some examples of calculation results on tower 170PNEM43.686 for r having values of 10^3, 10^5 and 10^7 Ω/m, respectively. A longitudinal cable resistance of 10^5 Ω/m can originate from either a surface resistivity of 4800 Ω or a volume resistivity of 0.066 Ωcm of the sheath, assuming the cable has a diameter of 15.4 mm and the sheath is 1.5 mm thick.

It is also possible to show, with this calculation method, how tracking occurs. Suppose the cable is wet with a relatively high conductivity. If a small piece of the cable is dry and therefore bad conducting, a high electrical field strenght in this dry zone will occur. Figure 4.2.2.5 and 4.2.2.6 show two possible situations.
Because of the calculation method that is used, the situations described in figure 4.2.2.5 and 4.2.2.6 are assumed to be symmetric around x=L. In both figures the resistance of the cable is 10^5 Ω/m. The 2 mm dry spot at x=30 has a resistance of 10^7 Ω/m in figure 4.2.2.5 and 10^9 Ω/m in figure 4.2.2.6. This results in an electric field strenght at x=30 of 0.08 kV/cm in figure 4.2.2.5 and 7 kV/cm in figure 4.2.2.6.

For controlling the voltage along the cable it could be possible to apply a better conducting layer inside the outer sheath of the cable. Because of the grounding through the capacitance layer-spiral the voltage and field strenght could be reduced depending on the conductivity of the layer. To calculate the voltage distribution in this situation the

model described in paragraph 4.2.1 has to be changed because the (more or less) conducting part of the cable is now not grounded directly at x=0 (tower), so V(x=0) ≠ 0. Assuming an infinite HV line with many towers, the system can be assumed symmetric around each tower. Then the boundary conditions are:

$$I(x=0) = 0 \equiv E(x=0) = 0$$
$$I(x=L) = 0 \equiv E(x=L) = 0$$

The results of this calculation are shown in figures 4.2.2.7 and 4.2.2.8, where the cable has a resistance of 10^5 Ω/m and 10^7 Ω/m respectively. From figure 4.2.2.7 we see that the voltage at 0<x<2 is in the order of 2.5 kV. This results in a high electric field strenght (20 kV/cm) between the conducting layer and the spiral because the insulating jacket is only 1.5 mm thick. A calculation with the finite element method would show the problems that can arise at the end of the spiral in this situation.

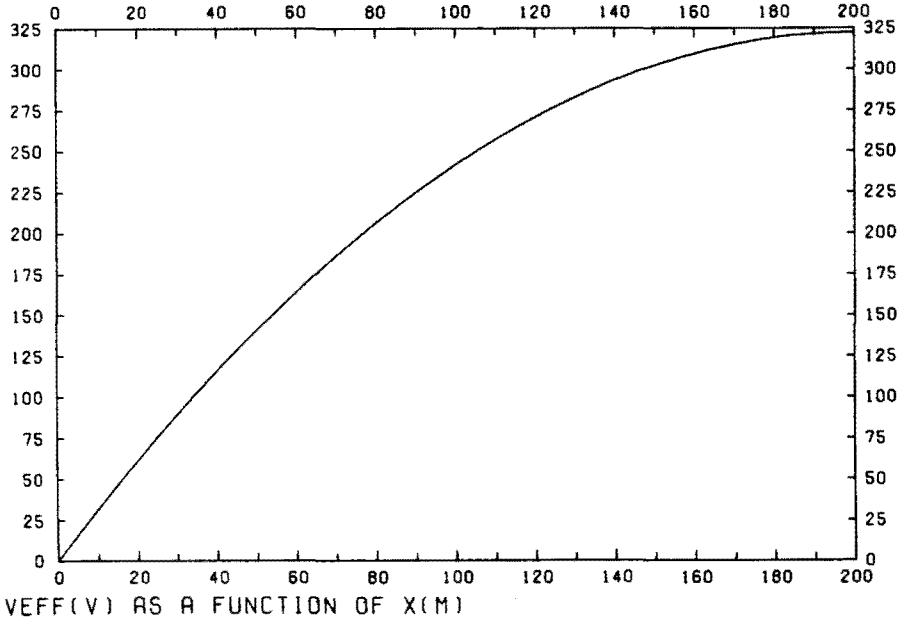

figure 4.2.2.2: r = 10^3 Ω/m;
E_{max} = E(x=0) = 3.22 V/m.

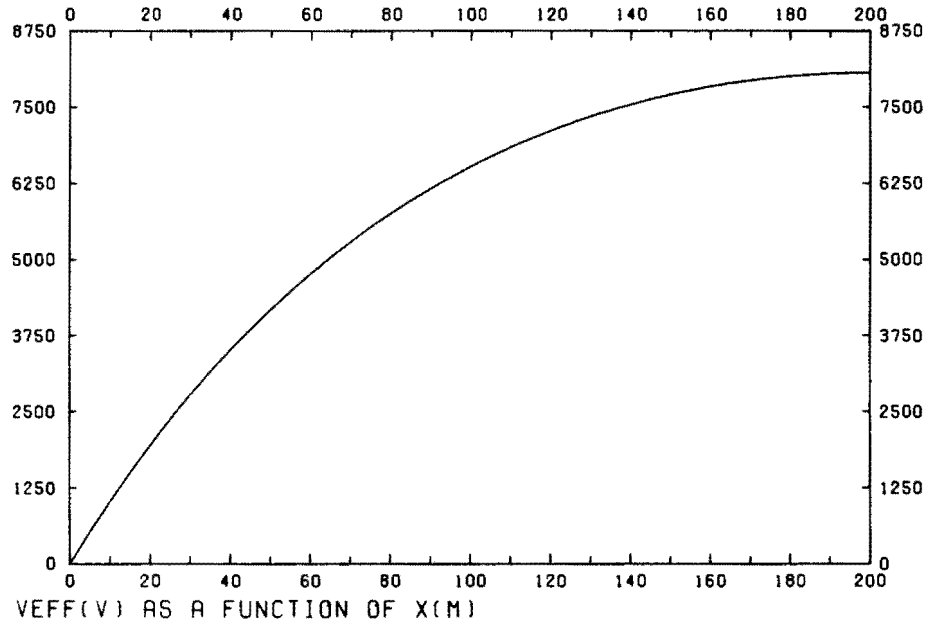

figure 4.2.2.3: r = 10^5 Ω/m;
E_{max} = E(x=0) = 107 V/m.

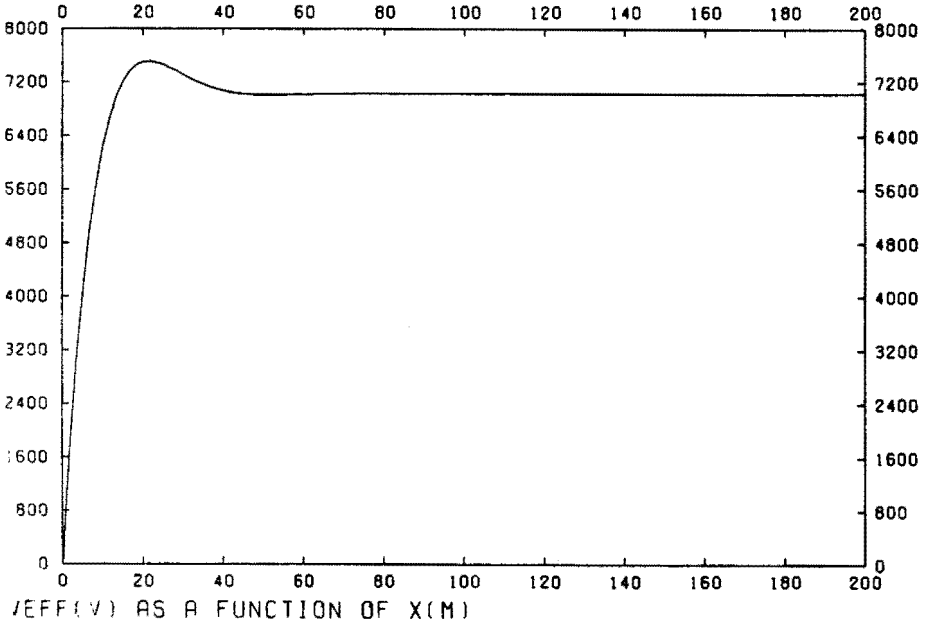

figure 4.2.2.4: r = 10^7 Ω/m;
E_{max} = E(x=0) = 1065 V/m.

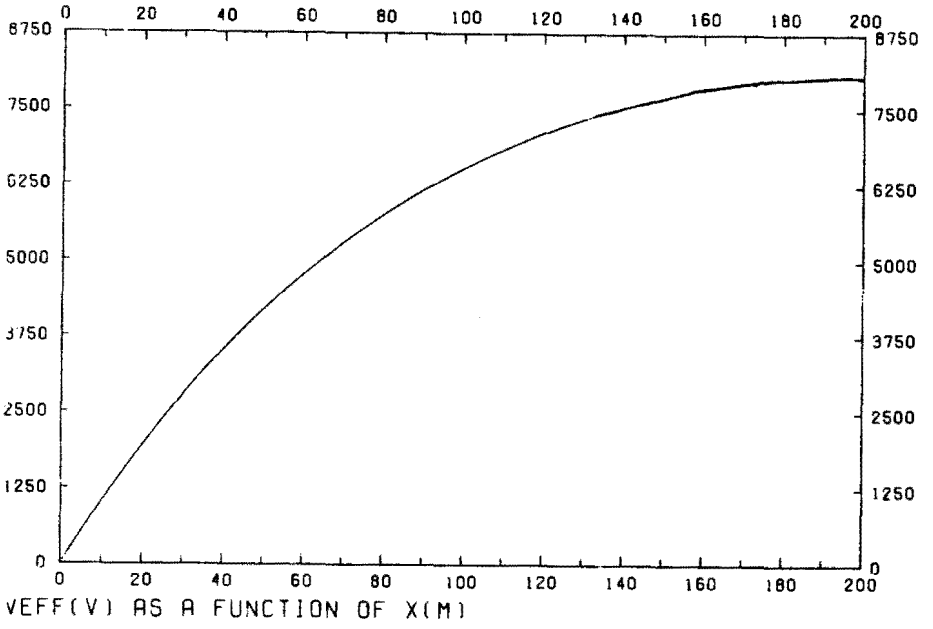

figure 4.2.2.5: Tracking, r = 10^5 Ω/m (10^7 Ω/m at x=30); E_{max} = E(x=30) = 0.08 kV/cm.

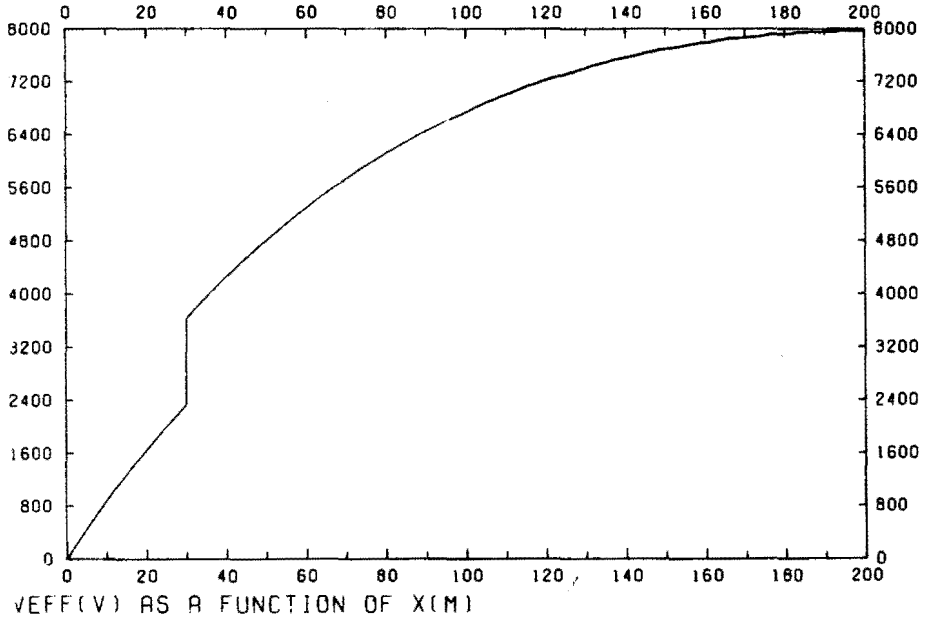

figure 4.2.2.6: Tracking, r = 10^5 Ω/m (10^9 Ω/m at x=30); E_{max} = E(x=30) = 7kV/cm.

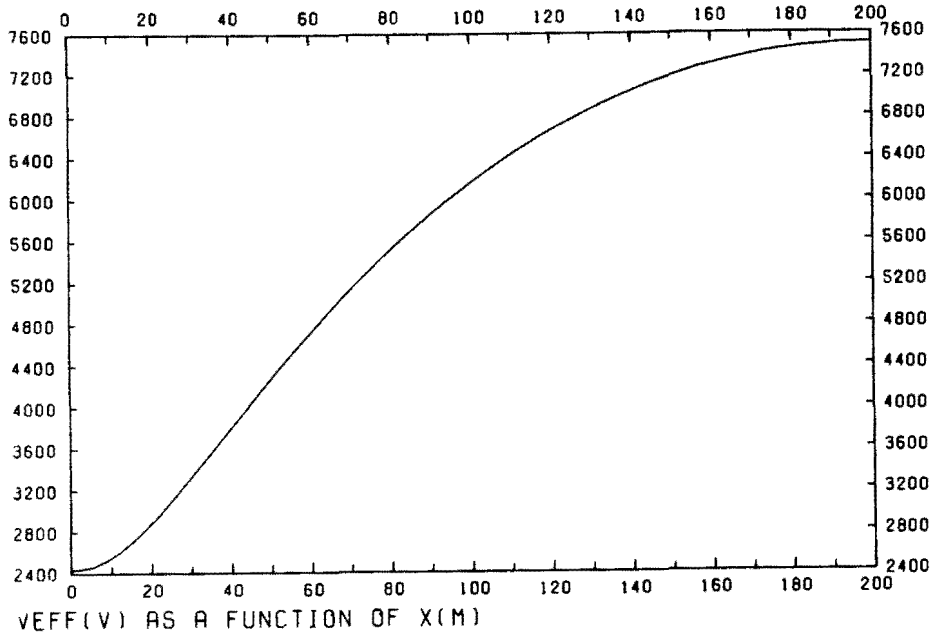

figure 4.2.2.7: $r = 10^5\ \Omega/m$;
$E_{max} = E(x=2) = 78\ V/m.$

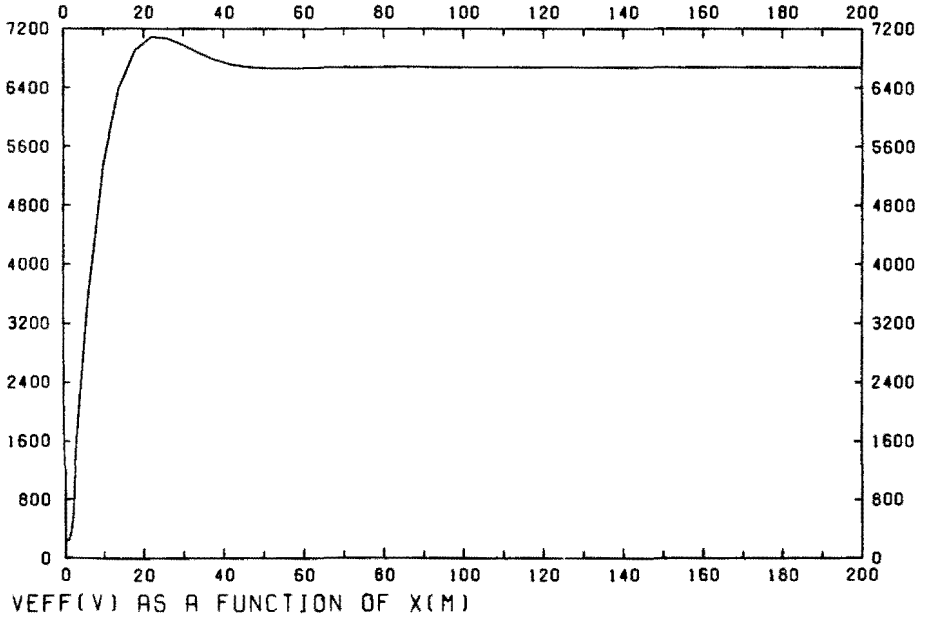

figure 4.2.2.8: $r = 10^7\ \Omega/m$;
$E_{max} = E(x=2) = 908\ V/m.$

4.3. FEM calculations

In order to illustrate the effect of field enhancement by the spiral-end, electric field strength calculations were performed using the Finite-Element-Method (FEM) [5,7]. The computer program that was used presumes a coaxial geometry. Because the optical fibre cable in the HV system may be assumed coaxial only very close to the cable, the calculation can only illustrate the effects at the end of the spiral.

Figure 1 shows the original situation and figure 2 shows a spiral-end which is shielded with a ring. The effect of the shielding can be evaluated by measuring the distance to the first equipotential line.

The cable is assumed to have the relative dielectric constant of PE, i.e. ϵ_r=2.3.

In both figures the grounded spiral shows triangles that are generated by the plotting program when the potential is very low. These triangles are the same as those generated as the computational mesh.

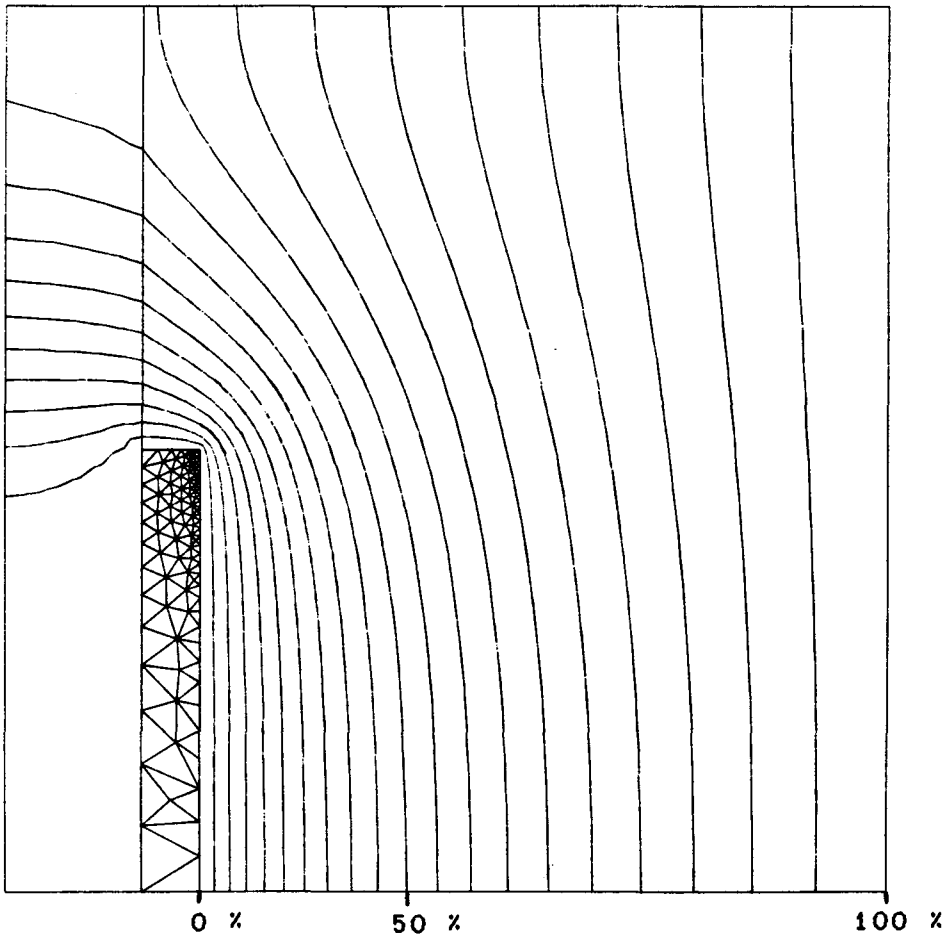

figure 4. 3. 1: Original spiral-end; equipotential lines at 5 % intervals.

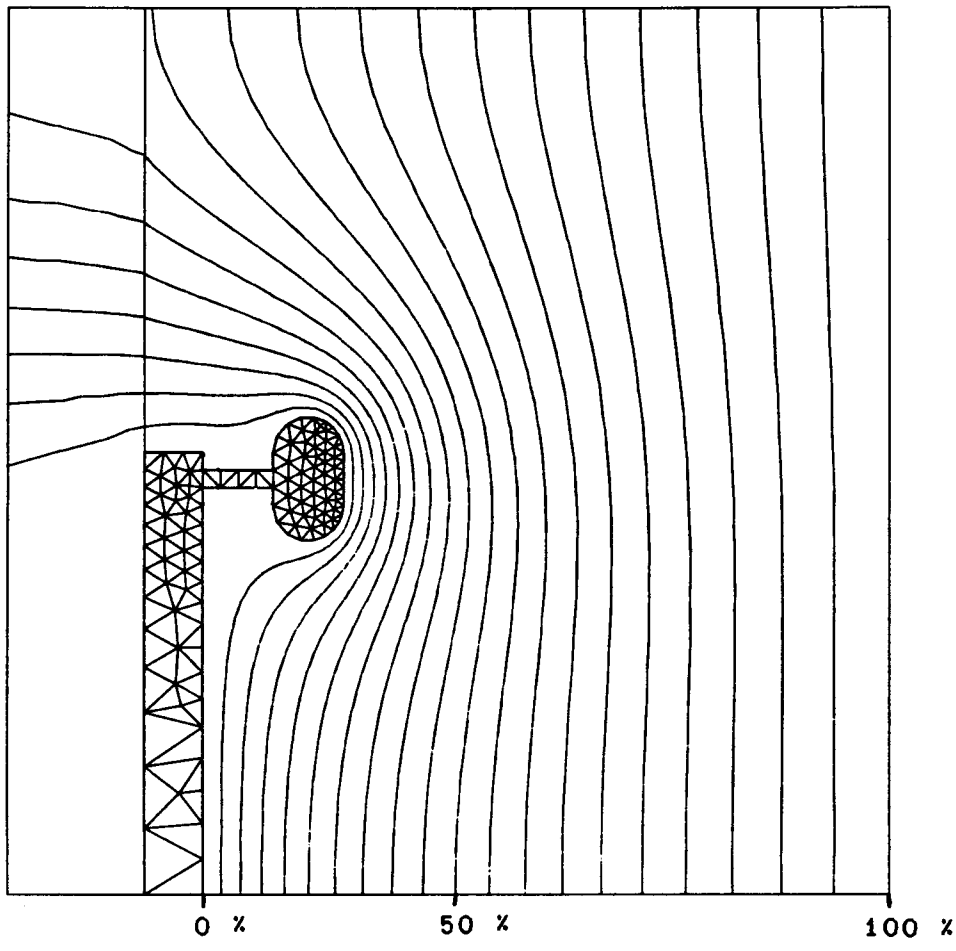

figure 4.3.2: Shielded spiral-end; equipotential lines at 5 % intervals.

5. Material property measurements

The material property measurements were performed on the following materials:

1. HDPE (DGDS 3420); sheath material of PNEM-cable
2. Megolon Si; copolymer filled with $Al(OH)_3$
3. 80%/20% mix of 2/1
4. 60%/40% mix of 2/1
5. LDPE (ALK 9211)
6. HDPE (Vest 5042)

5.1. Surface resistance

In this paragraph only the results of the surface resistance measurements are given. The complete report is given in appendix A.

specimen	surface resistivity σ (Ω)
2	$1.2 \cdot 10^{9}$
5	$1.7 \cdot 10^{10}$
3	$2.8 \cdot 10^{10}$
4	$5.1 \cdot 10^{10}$
1	$1.9 \cdot 10^{11}$
6	$8.7 \cdot 10^{11}$

table 5.1.1: Surface resistivities.

The results of the measurements on material nr. 2 are given in figure 5.1.1 as a function of the relative humidity.

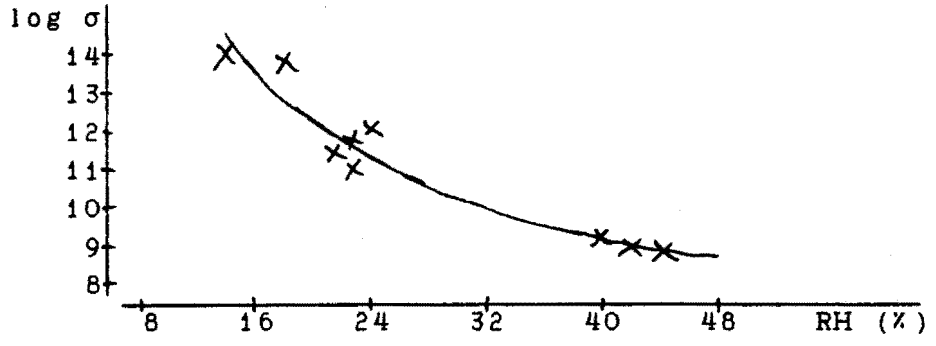

figure 5.1.1: Surface resistivity as a function of relative humidity.

Table 5.1.2 gives the the results of measurements performed elsewhere on UV aged samples. Resistivity was measured immediately after conditioning (>24 hours) at 100 % RH and 23 °C.

No information was given on the accuracy and the reproducibility of these measurements. Ageing usually results in a decrease of surface resistivity. The aged sample of material nr. 1 has a higher surface resistivity than the new one, this could not be explained.

specimen	σ (Ω, new)	σ(Ω, aged)
1	$2.0 \cdot 10^{13}$	$9.9 \cdot 10^{13}$
2	$3.5 \cdot 10^{10}$	$6.7 \cdot 10^{6}$

table 5.1.2: Resistivity of aged samples.

5.2. Tracking resistance

Tracking resistance was measured by KEMA on the materials 2 to 5. These tests were done in accordance with IEC publication 112 [1]. For all 5 materials the comparative tracking index (CTI) was determined in 3 tests using test solution B. This solution has a resistivity of 170 Ωcm and is more aggressive than the other solution, A (395 Ωcm). The CTI is defined as: the numerical value of the maximum voltage in volts at which a material withstands 50 drops without tracking. Failure is detected when a current of 0.5 A or more has persisted for 2 seconds. Tracking may occur during this test when voltage is applied between a defined electrode arrangement (figure 5.2.1) on the surface of a material and drops of electrolyte are applied between them at defined intervals of time (2 drops per minute). The number of drops needed to cause failure increases with the reduction of the applied voltage and, below a critical value, tracking ceases to occur. Figure 5.2.1 shows the measuring set up of IEC 112.

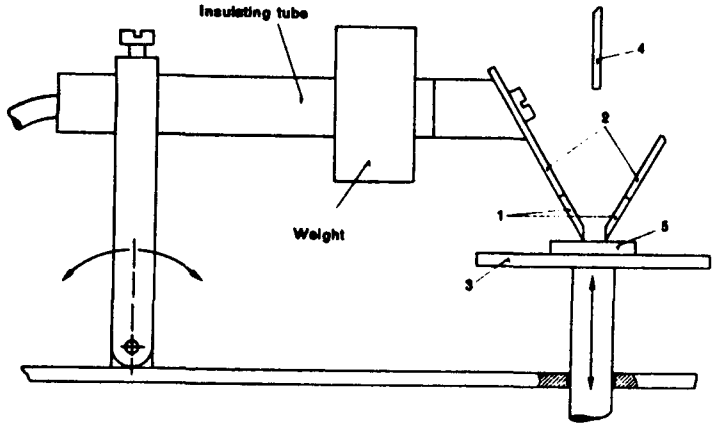

figure 5.2.1: Set up for tracking resistance tests.

All five materials withstood the test three times at 600 V, so they can be quallified with: CTI 600 M.

6. System property measurements

Building a laboratory setup with similar capacitance values as in paragraph 4.2.2 is not practicle because of the large distances required. It is possible, however, to built a setup in a laboratory with higher capacitances, that induces the same potential on the cable as in practical situations, using a lower source voltage. For this a brass tube of 8 cm diameter was used. The complete measuring set-up is displayed in figure 6.1 and 6.2. The lenght of the cable between the spirals (2L) is 2.17 m.

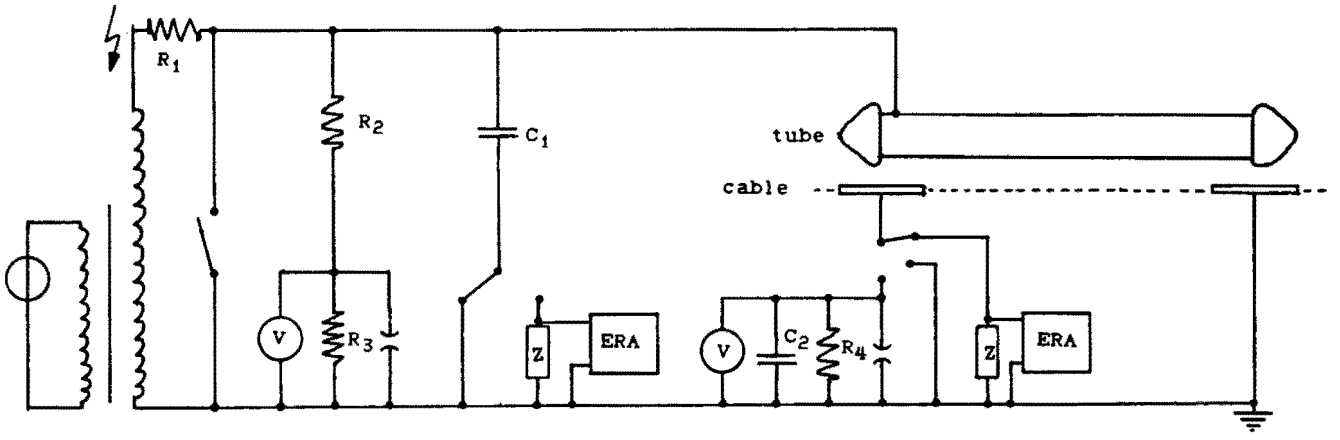

R_1 = 25 kΩ
R_2 = 1100 MΩ
R_3 = 10 kΩ
R_4 = 10 kΩ

C_1 = 99 pF
C_2 = 47 nF
Z: ERA measuring impedance

figure 6.1: Measuring circuit.

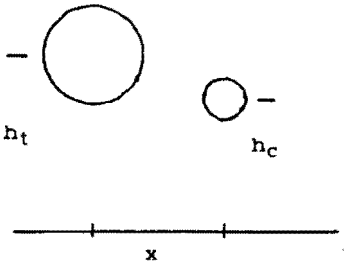

h_t = 383 mm
h_c = 304 or 287 mm
x = 128....195 mm

figure 6.2: Cable arrangement.

For the detection and analysis of the discharges an ERA Model 3 discharge detector was used together with a multi channel analyser. The system without cable was found to be free of discharges until 50 kV. The sensitivity of the discharge measurement is determined by the presence of internal and external noise. High sensitivity (0.3 pC apparant

charge) is possible when the ERA is connected to the spiral. When the ERA is connected to C_1, however, the whole HV circuit acts as an antenna and therefore the sensitivity is limited to about 10 pC.
The capacitances of the system in figure 6.2 were calculated with the method given in paragraph 4.1.1. They are

c_{te} = 15.2 pF/m (tube to earth)
c_{tc} = 6.9 pF/m (tube to cable)
c_{ce} = 8.0 pF/m (cable to earth)

when

h_t = 382 mm
h_c = 304 mm
x = 162 mm

The solution that is used for wetting the cable consists of 1 g NH_4Cl and 4 ml T-pol (wetting agent) in 1 l distilled water. The resistivity of this solution is 400±30 Ωcm. This solution resembles the ones used in the IEC tracking tests (IEC 112 and IEC 587).

6.1. Current.

The current to one spiral was measured in order to compare it with the calculations of paragraph 4.2. The calculated current, related to the source voltage, as a function of the cable resistance is given in figure 6.1.1.

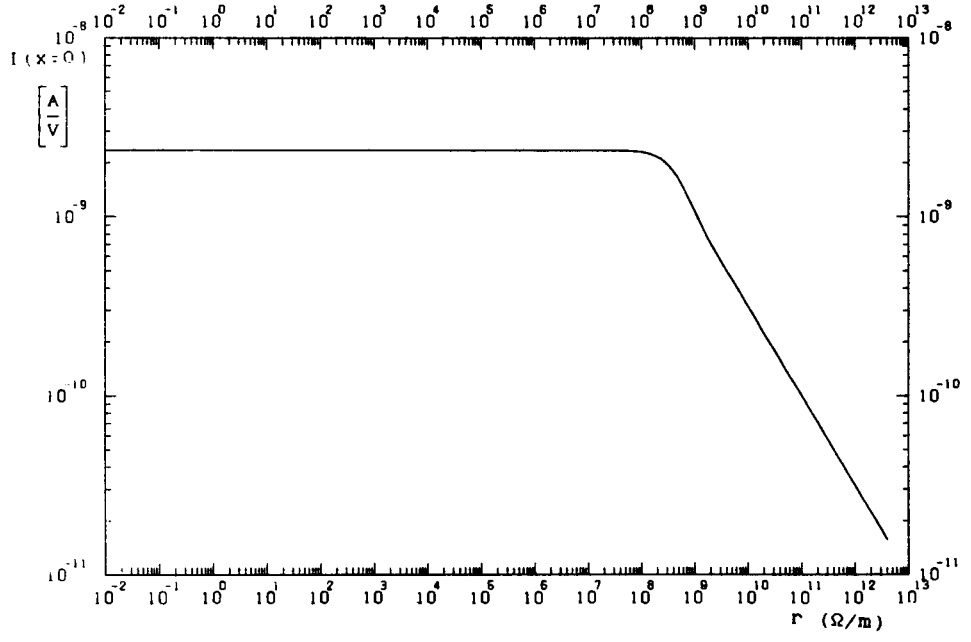

figure 6.1.1: Calculated current.

The measured current also contains a capacitive current from the source to the spiral. So this current should be measured and substracted from the other measurements. For this the cable was grounded close to the spiral-end (at a distance of about 5 mm). The measured currents are:

correction current $1.08 \cdot 10^{-9}$ A/V
dry cable $1.26 \cdot 10^{-9}$ A/V
wetted cable $3.2 \cdot 10^{-9}$ A/V

Thus the corrected values are:

dry cable $1.8 \cdot 10^{-10}$ A/V
wetted cable $2.1 \cdot 10^{-9}$ A/V

The current on the wetted cable is in accordance with figure 6.1.1 for $r < 2 \cdot 10^{8}$ Ω/m. The current on the dry cable indicates that $r \approx 3 \cdot 10^{10}$ Ω/m, which value is too low for a clean dry cable, see paragraph 5.1. An explanation for this can be found in the used model. At high values of r the longitudinal capacitance of the cable is probably more important than the resistance, whereas this capacitance is not included in the model. More experimental information may be derived from experiments at different frequencies.

6.2. Corona

The purpose of the corona measurements was to determine the corona onset voltage in different system configurations. From the corona onset voltages the maximum electric field strenght on the spiral can be calculated compared to the values given in paragraph 4.1.2. The different system configurations were obtainded by changing h_c and x within the margins given in figure 6.2.

The current pulses resulting from the discharges were measured between the spiral and ground, see figure 6.1. In each measurement, before recognizable[2] corona discharges started, other discharges, with a similar magnitude, occurred. These could not be recognized. Corona discharge pulses are spread symmetrically around the positive voltage peaks. Table 6.2.1 gives the results of these measurements.

h_c mm	x mm	V_1 kV	E_1 kV/cm	V_2 kV	E_2 kV/cm
304	151	25.0	3.94	29.5	4.65
304	128	24.5	4.39	27.5	4.93
304	162	28.8	4.29	31.5	4.69
287	195	31.0	3.77	41.0	4.99
287	179	37.5	4.89	40.0	5.22
287	153	34.3	5.04	35.8	5.26

V_1: discharge onset tube voltage
E_1: maximum electric field strenght on spiral at V_1
V_2: corona onset tube voltage
E_2: maximum electric field strenght on spiral at V_2

table 6.2.1: Corona onset.

Knowing the discharge field strength to be about 30 kV/cm,

the field strength enhancement factor related to the values E_1 of table 6.2.1 is about 7. Here the axial electric field strength is not taken into account, which is realistic for r values up to about 10^{12} Ω/m.
The field strength enhancement factor of the the spiral-end is not constant over the complete circumference. Also the condition of the surrounding air influences the onset voltage.
A typical discharge pattern of corona is shown in figure 6.2.1. The following values apply to this figure:

time (duration of measurement) = 200 s
tube voltage = 41 kV
h_c = 287 mm
x = 195 mm

The peak at the end of the scale (N = 6497) contains all discharges larger than 185 pC.

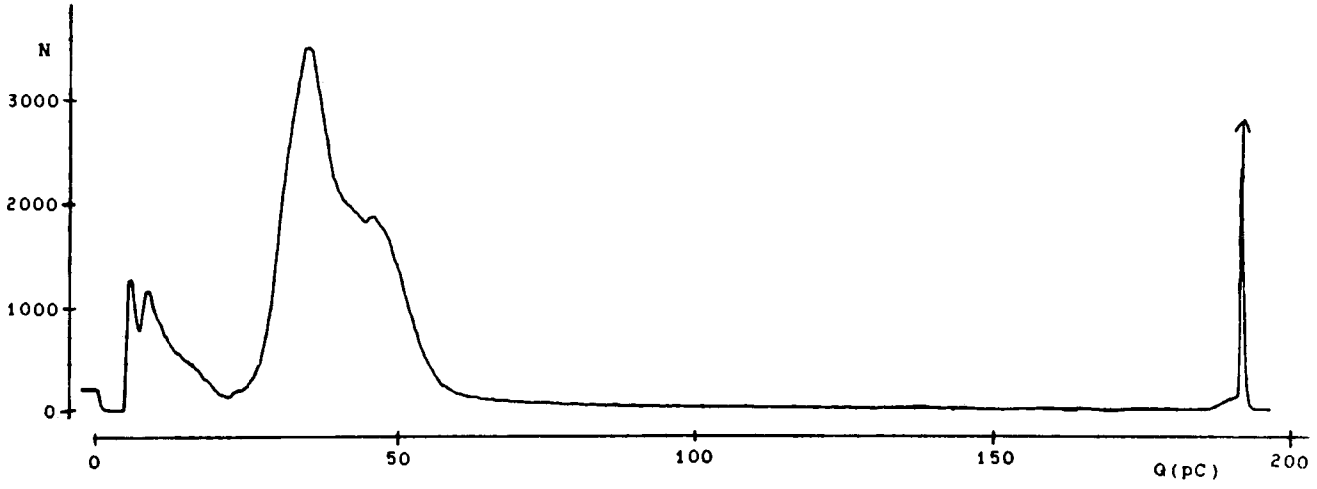

figure 6.2.1: Corona discharge pattern.

Shielding the spiral-ends would increase the corona onset voltage significantly; as can be seen in paragraph 4.3. Figure 6.2.2 shows the (copper) rings that were used for the shielding.

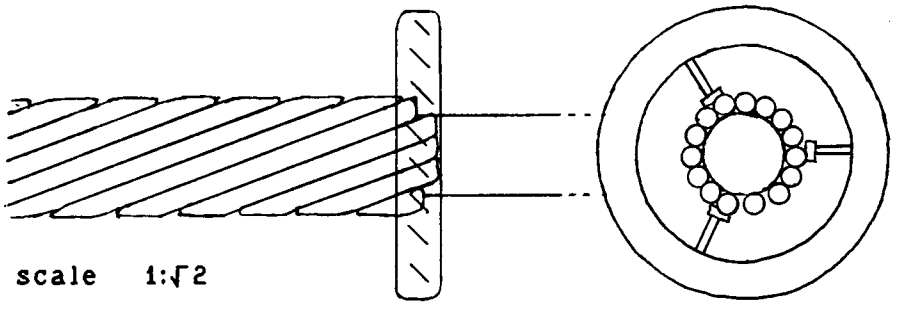

figure 6.2.2: Shielding ring.

After applying the rings it was not always possible to raise the voltage high enough for corona onset. The maximum vol-

tage was determined by the flashover probability between tube and spiral. In practice such a situation is not realistic because of the larger distances and smaller conductor sizes involved.
Occasionally corona pulses were observed, with shielding ring mounted. This resulted in a typical discharge pattern as in figure 6.2.3.

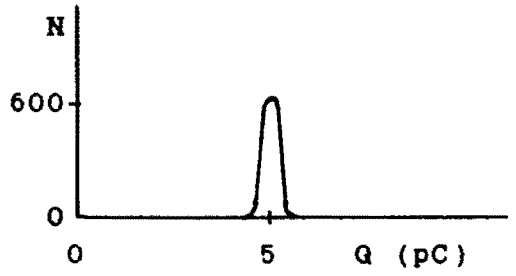

time = 200 s
tube voltage = 32.5 kV
h_c = 304 mm
x = 162 mm

figure 6.2.3: Corona on ring.

Although the measured (or apparant) charge may be smaller than the actual charge involved, discharge magnitudes of a few pC are considered harmless.

6.3. Insulated suspension

Insulated suspension was achieved by disconnecting one spiral from ground. The other one was grounded and shielded. Discharges were measured at the low voltage side of capacitor C_1 (figure 6.1). Discharges started at 30 kV and were recognized[2] as discharges from a floating metal object. Figure 6.3.1 shows a discharge pattern for this situation with

time = 200 s
tube voltage = 40 kV
h_c = 287 mm
x = 153 mm

Because of the different kind of discharge measurement, the amplification of the ERA had to be increased. This resulted in more noise. Therefore a bigger part of the lower side of the scale is surpressed.

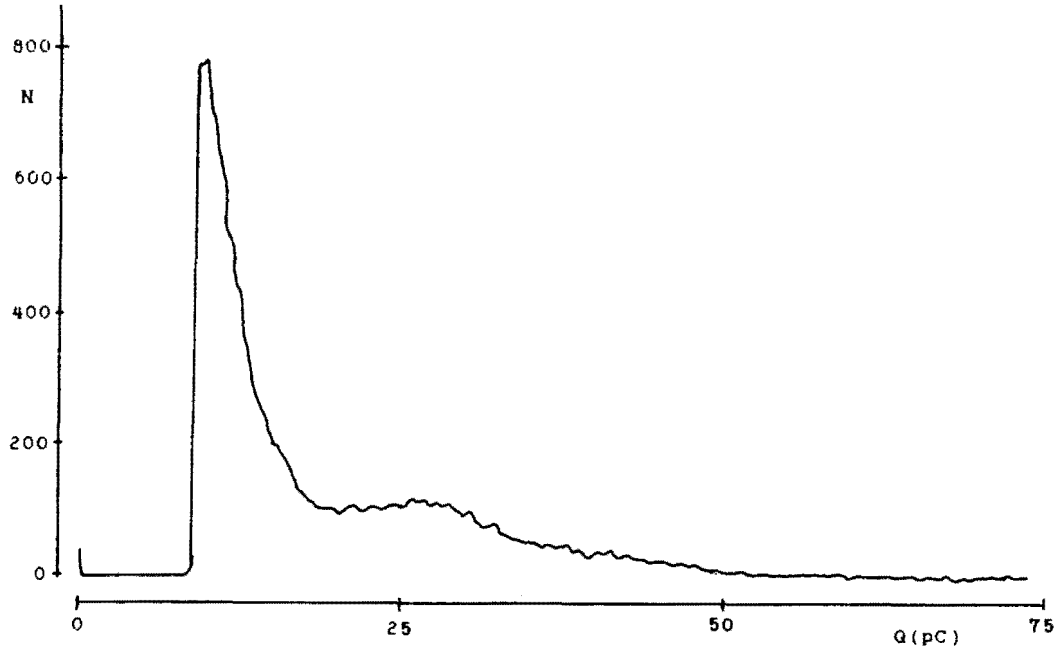

figure 6.3.1: Insulated suspension.

6.4. Tracking

Tracking discharges can be measured after checking that all other discharges are excluded by the shielding of the spiral-ends. Because the solution that is applied on the cable evaporated quickly, tracking could be observed for periods of only one to three minutes. The tracking discharges produced more sound than the corona discharges. The current pulses resulting from the discharges were measured between the spiral and ground, see figure 6.1.

Figure 6.4.1 shows tracking discharge patterns for two voltages.

continuous line: V_{tube} = 41 kV
dashed line: V_{tube} = 23 kV
time = 1000 s
h_c = 287 mm
x = 195 mm

figure 6.4.1: Tracking discharge pattern.

In both plots, the peaks at the end of the scale contain all discharges that are larger than 185 pC. Discharges started 200 s after applying voltage. Small discharges followed the large ones. After 400 s the discharges extinguished.

7. Discussion

Three electrical phenomena contribute to the ageing of an optical fibre cable:

1. corona
2. arcing/tracking
3. high currents in wet aramide strength members

ad 1. Corona can occur on the end of the suspension spiral and on the cable. Corona at the cable's surface may occur when it is conducting, and contains protruding irregularities on the surface. Whether corona occurs depends on the electric field strength on the spiral. Corona can be prevented either by choosing a suspension position with low electric field strength, or by shielding the spiral-end. The maximum unperturbed electric field strength at the spiral that can be tolerated is about 3 KV/cm. At this field strength the field enhancement of the spiral-end will not cause discharges. Shielding the spiral-end can not prevent corona on the cable surface. From the corona measurements it is not clear where the discharges take place, at a spot close to the cable, or at the outer side of the spiral. The latter will have less influence on the cable.

ad 2. Arcs resulting in tracks can also occur when the potential of the cable is low. Material properties influence the process in two ways:

- material properties have an influence on the occurrence of tracking
- material properties influence the possible damage when tracking occurs

The contributing material properties for the tracking phenomenon are:

- electrical conductivity of cable
- tracking resistance of the sheath material

A reduction of the occurrence of tracking can be obtained by reducing the axial electric field strength on the cable. The most important method for this is the choice of a low potential suspension position. Other methods are: reducing the resistivity of the cable sheath, applying a more conducting layer underneath the cable sheath and insulated suspension.

Reducing the cable resistivity from 10^9 Ω/m to 10^7 Ω/m reduces the axial field strength with about a factor 10 (the maximum axial electric field strength is approximately proportional to $\sqrt{r}$). Adding a large amount of carbon black to the sheath material will reduce the resistivity, but will also reduce the tracking resistance and some important mechanical properties. The aluminum hydroxide filled polymer

that was tested in paragraph 7.1 has a lower surface resistivity than HDPE. However, because the reduction is small and because this material's other properties are inferior, it is not considered as an alternative.
The second method, the addition of a layer with a higher conductivity underneath the cable sheath, can give rise to the problems already described in paragraph 4.2, i.e. a high radial electric field strength depending on the resistivity of the layer. When properly designed however these fields are harmless.
The axial field strength reduction obtained with insulated suspension is about a factor 10.
The damage caused by tracking can be decreased by choosing a more tracking resistant sheath material. The IEC 112 test method is not severe enough for the comparison of new sheath materials with the original, see paragraph 7.1. A better test method is the "inclined-plane tracking" test method (ASTM D2303, IEC 587).
ad 3. The maximum power dissipation in/on the cable at the tower, p(x=0), is always smaller than 1 W/m, so no damage is expected. The sudden grounding of the wet (conducting) cable could result in higher current impulses. No calculations were made on this subject but it is expected that the impulses are damped by the capacitances involved.

Tracking discharges show a larger charge, but appear at a lower rate, than corona discharges. Therefore from the measurements it can not be concluded that tracking is more important for the deterioration of the cable than corona. However, in literature tracking is seen as the most important problem for metal free optical fibre cables. Comparing the tracking with the corona measurement results, it can be seen that in practical tracking situations (i.e. continuous wetting and drying) larger discharges are present than with corona. Because tracking produces irregularities on the cable surface, subsequent tracking will often take place on the same spots.

Possible electrical failure situations that can damage the cable are:

- cable touches phase wire
- impulse voltages (resulting from switching or lightning) on phase or ground wire
- lightning strike on cable

In situations where the cable has a high resistance the first gives the same results as given in figure 4.2.4/1 where V_p is now the phase voltage.
The impulse voltages have components of high frequency and therefore the parameter γ will be higher.

Resuming, proposals for modifications and further research are:

1. Installation of a part of an optical fibre cable with correctly dimensioned insulators (about 20 kV) in about 5 successive towers makes it possible to compare both types of installation after a few years of service.
2. Shielding rings should be mounted on the spiral-ends not only when the radial field strength can be high, because failure situations may result in a much higher field strength.
3. A more conductive jacket which has high tracking resistance offers many advantages, but is not yet available. More research is needed therefore.
4. Applying a conductive layer underneath the jacket separates the requirements for conductivity and tracking resistance, but can result in high radial electric field strength. An optimal value for the resistivity should be found.

8. Conclusions

The calculation of the potential distribution perpendicular to the optical fibre cable is possible using the line charge simulation method. These calculations can give information about the choice of a suspension position, radial electric field strength's and capacitances between wires, cable and ground.

The calculation of the potential distribution along the cable is only usefull for cable resistivities that are not too high. Measurements indicated that the model that is used is not accurate for high resistivities (10^{10} Ω/m or higher).

The measurement of high surface resistivities is difficult. The method used in this report was accurate enough for the comparison of the different materials.

In laboratory experiments it was possible to visualize and measure corona and tracking discharges separately.

Tracking was found to be the most serious electrical mechanism that can deteriorate the optical fibre cable. Corona can also cause damage to the cable surface, close to the end of the suspension spiral.

Tracking can be reduced by choosing a low potential suspension place, increasing the conductivity of the sheath, applying a conductive layer underneath the sheath and by insulated suspension. The choice of a tracking resistant sheath material reduces the damage caused by the arcs on the cable surface.

Corona at the spiral-ends can be prevented by choosing a suspension place where the radial electric field strength on the spiral is low, and by shielding the spiral-ends.

9. References

Chapter 1.

1. Brüggendieck, S. et al.
   25 KM OPTICAL AERIAL CABLE LINK ON 110 KV OVERHEAD LINE.
   CIGRE, 1984, 35-09
2. Haag, H. G. and P. E. Zamzow
   LUFTKABEL MIT LICHTWELLENLEITERN.
   etz, Vol. 106(1985), No. 4, p. 154-160
3. OPTICAL FIBRE CABLE FOR AERIAL APPLICATION IN HIGH VOLTAGE NETWORKS.
   brochure, NKF Telecommunication Cable Systems, Waddinxveen, Holland, 1986.
4. IEEE, 83 WM 025-4
   FIBER OPTIC APPLICATIONS IN ELECTRICAL SUBSTATIONS.
   IEEE Microwave Radio Subcommittee & Research Subcommittee of the Power System Communication Committee

Chapter 2.

1. ASTM D1711-79a
   STANDARD DEFINITIONS OF TERMS RELATING TO ELECTRICAL INSULATION.
   1980 Annual book of ASTM standards, part 39
2. Kuffel, E. and W. S. Zaengl
   HIGH VOLTAGE ENGINEERING.
   Oxford: Pergamon, 1984

Chapter 3.

1. Brüggendieck, S. et al.
   25 KM OPTICAL AERIAL CABLE LINK ON 110 KV OVERHEAD LINE.
   CIGRE, 1984, 35-09
2. Chandler, R. L. J. et al.
   STRESS CORROSION FAILURE OF COMPOSITE LONG ROD INSULATORS.
   Fourth Int. Symp. HV Eng., Athens, 1983, 23.09
3. Cojan, M. et al.
   POLYMERIC TRANSMISSION INSULATORS: THEIR APPLICATION IN FRANCE, ITALY AND U. K.
   CIGRE, 1980, 22-10
4. El-Arabaty, A. et al.
   AGEING OF HV EPOXY RESIN INSULATORS UNDER SERVICE CONDITIONS AND ITS EFFECTS ON THEIR ELECTRICAL CHARACTERISTICS.
   Third Int. Symp. HV Eng., Milan, 1979, 23.01
5. Cortina, R. et al.
   DIAGNOSTIC TECHNIQUES TO EVALUATE THE PERFORMANCE OF POLYMERIC INSULATORS.

Fourth Int. Symp. HV Eng., Athens, 1983, 22.12

6. Weihe, H. et al.
FIELD EXPERIENCE AND TESTING OF NEW INSULATOR TYPES IN SOUTH AFRICA.
CIGRE, 1980, 22-03

7. SERVICE EXPERIENCE WITH THE GERMAN COMPOSITE LONG ROD INSULATOR WITH SILICONE-RUBBER SHEDS.
CIGRE, 1980, 22-11

8. El-Arabaty, A. et al.
EFFECTS OF INSULATOR SHAPE DIMENSIONS AND MATERIAL ON ITS FLASHOVER CHARACTERISTICS.
Fourth Int. Symp. HV Eng., Athens, 1983, 46.04

9. Steinort, E.
SURFACE DEFECTS OF FILLED EPOXY RESINS CAUSED BY IRRADIATION AND PARTIAL DISCHARGE STRESS.
Third Int. Symp. HV Eng., Milan, 1979, 23.08

10. Kärner, H. et al.
TRACKING AND EROSION OF POLYMERIC INSULATING MATERIALS FOR OUTDOOR APPLICATION.
Third Int. Symp. HV Eng., Milan, 1979, 23.09

11. El-Arabaty, A. et al.
MEASUREMENT OF TEMPERATURE OF HIGH-VOLTAGE POLLUTED INSULATORS USING INFRA-RED TECHIQUES.
Third Int. Symp. HV Eng., Milan, 1979, 54.02

12. Kind, D. and H. Kärner
HOCHSPANNUNGS-ISOLIERTECHNIK.
Braunschweig/Wiesbaden: Vieweg, 1982.

13. Müller, B.
BEHAVIOUR OF ORGANIC INDOOR INSULATION UNDER ELECTRICAL AND CLIMATIC STRESSES.
Fourth Int. Symp. HV Eng., Athens, 1983, 46.06

14. OPTICAL FIBRE CABLE FOR AERIAL APPLICATION IN HIGH VOLTAGE NETWORKS.
brochure, NKF Telecommunication Cable Systems, Waddinxveen, Holland, 1986.

15. Blahma, J. et al.
LICHTWELLENLEITER-EINSATZ IN DER ENERGIEVERSORGUNG.
etz, Vol. 106(1985), No. 4, p. 174-177

16. private communication at NKF.

17. Haag, H.G. and P.E. Zamzow
LUFTKABEL MIT LICHTWELLENLEITERN.
etz, Vol. 106(1985), No. 4, p. 154-160

18. Mark, H.F. (editor)
ENCYCLOPEDIA OF POLYMER SCIENCE AND TECHNOLOGY
Vol. 6, p. 275 - 313
Interscience Publishers, New York, 1967

19. ASTM D495-73
HIGH-VOLTAGE, LOW-CURRENT, DRY ARC RESISTANCE OF SOLID ELECTRICAL INSULATION.

1980 Annual book of ASTM standards, part 39

20. Parr, D. J. and R. M. Scarisbrick
PERFORMANCE OF SYNTHETIC INSULATING MATERIALS UNDER POLLUTED CONDITIONS.
Proc. IEE, Vol. 112(1965), No. 8, p. 1625 - 1632

21. IEC Publication 112, Third edition, 1979
METHOD FOR DETERMINING THE COMPARATIVE AND THE PROOF TRACKING INDICES OF SOLID INSULATING MATERIALS UNDER MOIST CONDITIONS.

22. ASTM D2132-68(1979)
DUST-AND-FOG TRACKING AND EROSION RESISTANCE OF ELECTRICAL INSULATING MATERIALS.
1980 Annual book of ASTM standards, Part 39

23. Clabburn R. J. T. et al.
THE OUTDOOR PERFORMANCE OF PLASTIC MATERIALS USED AS CABLE ACCESSORIES.
IEEE Trans. on PAS, Vol. PAS-92(1973), p. 1833 - 1842

24. ASTM D2303-73(1979)
LIQUID-CONTAMINANT, INCLINED-PLANE TRACKING AND EROSION OF INSULATING MATERIALS. (equivalent to IEC 587)
1980 Annual book of ASTM standards, Part 39

25. McNicoll, Y. et al.
CONTACT ANGLE MEASUREMENTS IN POLYETHYLENE AND HIGH-VOLTAGE EXTRUDED CABLES.
IEEE Conf. Rec. of 1983 Interfacial phenomena in practical insulating systems, Gaithersburg, Sept. 19-20, 1983, p. D1

26. Field, R. F.
THE FORMATION OF IONISED WATER FILMS ON DIELECTRICS UNDER CONDITIONS OF HIGH HUMIDITY.
Journal of Applied Physics, Vol. 17(1946), p. 318-325

27. Licari, J. J.
PLASTIC COATINGS FOR ELECTRONICS
New York: McGraw-Hill Book Company, 1970

28. Nagofis, I. M.
PLASTICS INSULATING MATERIALS
Princeton: P. Van Nostrand, 1966

29. Gross, S. (editor)
MODERN PLASTIC ENCYCLOPEDIA
New York: McGraw-Hill, 1971

30. Gilroy, H. M.
POLYOFIN LONGITIVITY FOR TELEPHONE SERVICE.
ANTEC 1985, p. 258 - 260

31. Stimper, K. and W. H. Middendorf
MECHANISMS OF DETERIORATION OF ELECTRICAL INSULATION SURFACES.
IEEE Trans. on El. Ins., Vol. EI-19(1984), No. 4, p. 314 - 320

32. IEC Publication 93, second edition, 1980

METHODS OF TEST FOR VOLUME RESISTIVITY AND SURFACE RESISTIVITY OF SOLID ELECTRICAL INSULATING MATERIALS.

33. IEC Publication 587, second edition, 1984
TEST METHODS FOR EVALUATING RESISTANCE TO TRACKING AND EROSION OF ELECTRICAL INSULATING MATERIALS USED UNDER SEVERE AMBIENT CONDITIONS.

34. Lewis, J. et al.
PRE-BREAKDOWN AND BREAKDOWN PHENOMENA ALONG PMMA SURFACES IN VACUUM AND NITROGEN GAS STRESSED BY 60 HZ VOLTAGES.
IEEE Trans. on El. Ins., Vol. EI-19(1984), No. 6

35. Kuffel, E. and W. S. Zaengl
HIGH VOLTAGE ENGINEERING.
Oxford: Pergamon, 1984

36. Barlett, et al.
THE DEVELOPMENT OF OPTICAL COMMUNICATION SYSTEMS IN THE UNITED KINGDOM ELECTRICITY SUPPLY INDUSTRY.
9th Int. Conf. on Electricity Distribution: CIRED 1987, Liège, Belgium, d. 12. 1

37. FIBER OPTIC AERIAL CABLES IN HIGH-VOLTAGE-LINES.
Siemens report, NK 8506 E LWL 1

Chapter 4.

1. Zaffanella, L. E. and D. W. Deno
ELECTROSTATIC AND ELECTROMAGNETIC EFFECTS OF ULTRA HIGH VOLTAGE TRANSMISSION LINES.
EPRI EL-802, Project 566, Final Report, june 1978
Palo Alto, Ca.: Electric Power Research Institute

2. Hochrainer, A.
SYMMETRISCHE KOMPONENTEN IN DREHSTROMSYSTEMEN.
Berlin: Springer, 1957

4. Flosdorff, R. and G. Hilgarth
ELEKTRISCHE ENERGIEVERTEILUNG.
Stuttgart: B. G. Teubner, 1973

5. Koelman, J. M. V. A.
FINITE ELEMENTS IN ELECTRIC FIELD PROBLEMS.
Group EHO, Dept. of Electrical Engineering, Eindhoven University of Technology, 1983
stageverslag EH. 83. S. 181

6. Kuepfmueller, K.
EINFUEHRUNG IN DIE THEORETISCHE ELEKTROTECHNIK.
Berlin: Springer, 1984

7. Kuffel, E. and W. S. Zaengl
HIGH VOLTAGE ENGINEERING.
Oxford: Pergamon, 1984

Chapter 6.

1. IEC Publication 112, Third edition, 1979
METHOD FOR DETERMINING THE COMPARATIVE AND THE PROOF

TRACKING INDICES OF SOLID INSULATING MATERIALS UNDER MOIST CONDITIONS.

2. RECOGNITION OF DISCHARGES.
CIGRE, Electra No. 11, 1969, Working Group 21.03

Appendix A: Surface resistance measurements

1. Introduction

From model and literature study it was found that surface resistance is an important material property[A1]. For this reason the surface resistance of 6 different materials has been measured. These materials are:

1. HDPE (DGDS 3420); sheath material of PNEM-cable
2. Megolon S1; copolymer filled with $Al(OH)_3$, expected to have a lower surface resistance than PE
3. 80%/20% mix of 2/1
4. 60%/40% mix of 2/1
5. LDPE (ALK 9211)
6. HDPE (Vest 5042)

At NKF some measurements were done on aged samples of the specimens 1 and 2.
The measurements were performed with help of IEC standard 93[A2].
Surface resistance cannot be measured accurately, only approximately, because more or less volume conductance is nearly always involved in the measurement. The measured value depends to a large extend on the contamination of the surface of the specimen at the time of measurement. However, the dielectric constant (e.g. polarisation) of the specimen influences the deposition of contaminants, and their conductive capabilities are effected by the surface characteristics of the specimen. Thus the surface resistivity is not a bulk material property, but can be considered to be related to material properties when contamination is involved.
Surface resistance, especially when high, often changes in an erratic manner, and in general depends strongly on the time that the voltage is applied to the specimen; this time is called electrification time.

2. Measuring method

Resistance was measured by measuring simultaneously the direct voltage applied to the unknown resistance and the current through it (voltmeter-ammeter method). The measuring circuit is shown in figure 1.

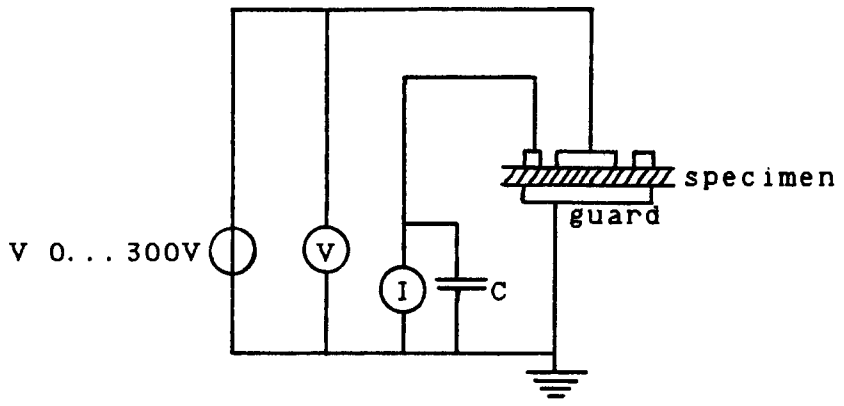

apparatus:
- DC source: EH911 PS53
- Voltmeter: Keithley 177 microvolt DMM
- Ammeter: Keithley 610C solid state electrometer
- Dewpoint: Endress + Hauser, hydrolog WMY 170
- Temperature: mercury thermometer
- wires: extra teflon insulated
- C: 1...100 nF

figure 1: Measuring circuit.

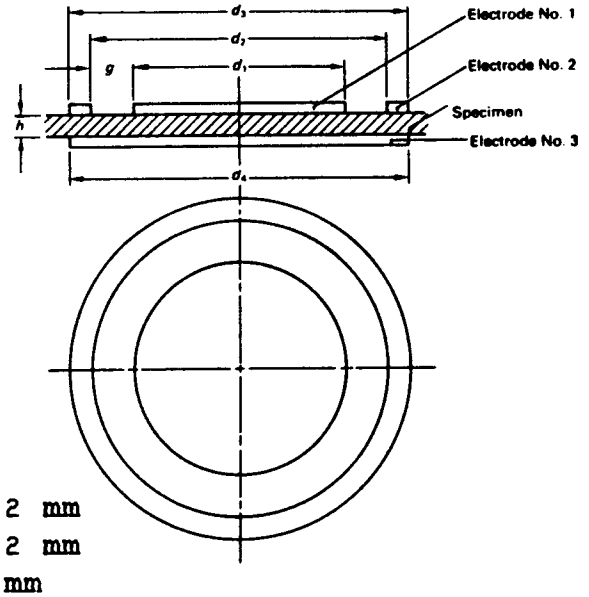

with d_1 = 50±0.2 mm
d_2 = 60±0.2 mm
d_3 = 70±3 mm
d_4 = 70±3 mm
All specimen were 3±0.3 mm thick

figure 2: Electrodes.

Before attaching the electrodes the specimen were cleaned with dry, dustfree, cleaning tissue paper and not touched anymore.
The electrodes were attached by sticking a plastic mould on

the specimen and painting silver paint on it. When the paint was dry, the mould was pulled off, leaving no traces behind. This method of electrode attaching gave very accurate electrode sizes for all specimen, see figure 2.
During the measurement the specimen was placed on a clean teflon structure, see figure 3.

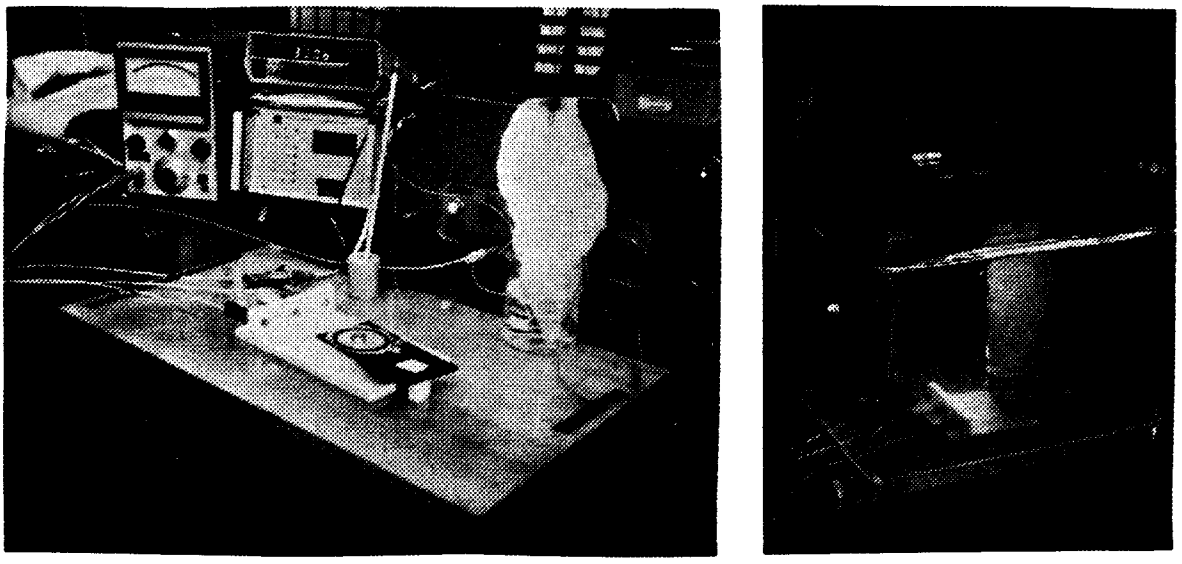

figure 3: Measurement set-up.

The capacitance applied to the input receptical of the ammeter damped out several kinds of low frequency oscillations, most of them resulted from moving things in the neighbourhood of the wires. A changing capacitance is created then, giving rise to a displacement current, d(CV)/dt.

Simultaneously with current and voltage the characteristics of the surrounding air were measured, i.e. temperatue and dew point. Normal and moistened climate was used. The moist climate was created by placing a glass cap over the specimen and a container with water. In the water some filtrating paper accelerated the evaporation. Because of changes in the outside temperature and humidity, relative air humidities (RH) were measured from 14% to 47%.

The measurements at NKF were done with a "megohm" meter with electrodes of slightly different sizes. The samples were aged by intense UV light comparable with 6.5 years of middle European sunlight.

3. Results

The surface resistivity is calculated with the following formula:

$$\sigma = R_X \frac{\pi(d_1+g)}{g} \qquad (3.1)$$

where:
σ is the surface resistivity (not to be interpreted as conductivity) in ohms, or Ωm/m
R_X is the measured (surface) resistance
$\pi(d_1+g)$ is the effective perimeter in metres of the guarded electrode
g is the distance in metres between the electrodes

The results of the complete set of measurements are given in table 5. In that table the parameter ∂ gives an indication about the relation resistivity/voltage. The parameter is defined as:

$$\partial = \frac{R_{75\ V}}{R_{300\ V}} \qquad (3.2)$$

The logarithmic mean values at RH = 43±2 % are given in table 2. Only resistivities measured at long enough electrification times are used for this table. The electrification times until steady state current are given in table 1.

specimen	time (min.) for steady state	(±%) current
1	--	--
2	30	5
3	40	10
4	100	5
5	100	5
6	180	13

table 1: Electrification times until steady state current.

specimen	surface resistivity σ (Ω)
2	$1.2 \cdot 10^{9}$
5	$1.7 \cdot 10^{10}$
3	$2.8 \cdot 10^{10}$
4	$5.1 \cdot 10^{10}$
1	$1.9 \cdot 10^{11}$
6	$8.7 \cdot 10^{11}$

table 2: Surface resistivities.

The results of the measurements on specimen nr. 2 are given in figure 4 as a function of the relative humidity.

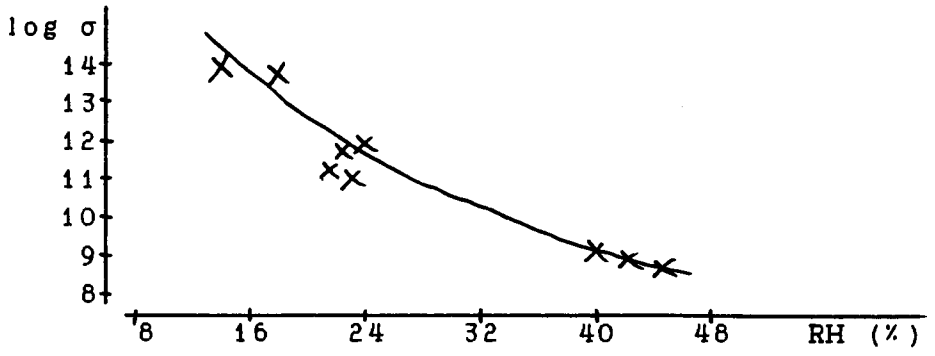

figure 4: Surface resistivity as a function of relative humidity.

The measurements done at NKF are reported in table 5. Resistivity was measured immediately after conditioning (>24 hours) at 100 % RH and 23 °C.
No information was given on the accuracy and the reproducibility of these measurements. Ageing usually results in a decrease of surface resistivity. The aged sample of material nr. 1 has a higher surface resistivity than the new one, this could not be explained.

specimen	σ (Ω, new)	σ(Ω, aged)
1	$2.0 \cdot 10^{13}$	$9.9 \cdot 10^{13}$
2	$3.5 \cdot 10^{10}$	$6.7 \cdot 10^{6}$

table 5: NKF measurements.

4. Reproducibility and accuracy

The error sources are:
1. error in voltage
2. error in current
3. error in dew point
4. error in temperature
5. error in electrode sizes
6. contact potential
7. contact resistance
8. leakage current
9. time of electrification

ad 1. The maximum relative error in the voltage measurement is 1 %.
ad 2. The maximum relative error in the current measurement is 2 %.
ad 3. The maximum absolute error in the dew point is 1

degree.

ad 4. The error of the thermometer is not known; it could be read with an accuracy of 0.2 degree.

ad 5. The width of all moulds was measured on 6 places spread over the circumference. In table 1 the results for each specimen are given.

specimen	$g = \langle d_1 - d_2 \rangle$ (mm)	μ (mm)	
1 S	5.43	0.07	
2 A	5.27	0.10	
2 S	5.38	0.12	
3 S	5.37	0.11	A = aquadag
4 S	5.49	0.09	S = silver
5 S	5.46	0.13	paint
6 S	5.39	0.09	

table 3: Mould sizes.

ad 6. To check the contact potential, current was measured with different ammeter-settings resulting in different voltages accross the ammeter. An eventually present contact potential was found to be smaller than 0.01 V and therefore could not influence the measurement.
this way.

ad 7. It is very difficult to check the measurement for contact resistance. Norman[A3] states that contact resistance varies with the resistivity of the sample, the type of contact, the applied voltage and the mechanical pressure. The influence of the type of contact could be checked by attaching also an aquadag (graphite) electrode on the specimen 1 and 2. The measurements with the aquadag electrodes did not differ from the measurements with silver paint electrodes.

ad 8. Leakage current was minimized by using extra insulated wires and a guarding electrode on the specimen, see figure 2. The effect of leakage current was checked by measuring the resistance of the complete circuit without specimen. This resistance was higher than 10^{14} Ω. The highest measured resistance was $9 \cdot 10^{12}$ Ω.

ad 9. The influence of the electrification time was examined by recording the current at constant voltage as a function of time. In that way the time for a steady state value of the current could be determined.

From the above described error sources no over-all accuracy of the measurements can be concluded. IEC standard 93[A2] prescribes an accuracy of the measuring device of 10 % for resistances below 10^{12} Ω, and 20 % for higher values. The accuracy of the measuring device can be determined from

the points 1, 2, 5, and 8 with help of equation 3.1.

$R_X(\Omega)$	rel. error
10^{12} - 10^{13}	15 %
10^{11} - 10^{12}	7 %
< 10^{11}	6 %

table 4: Measuring device error.

Because of the variability (spread) of the resistance of a given specimen with test conditions determinations are[A2] usually not reproducible to closer than ±10 % and are often even more widely divergent (a range of values of 10 to 1 may be obtained under apparently identical conditions).
The reader can get an idea of the reproducibility of the measurements on one specimen by looking at the complete set in appendix 1.
With help of point 3 and 4 the error in the relative humidity can be determined. This leads to a relative error of 8 %.

5. References

A1. FIBER OPTIC AERIAL CABLES IN HIGH-VOLTAGE-LINES.
Siemens Report, NK 8506 E LWL 1

A2. IEC Publication 93, second edition, 1980
METHODS OF TEST FOR VOLUME RESISTIVITY AND SURFACE RESISTIVITY OF SOLID ELECTRICAL INSULATING MATERIALS.

A3. Norman, R. H.
CONDUCTIVE RUBBERS AND PLASTICS.
London: Applied Science Publishers, 1970

Specimen	Meas. Nr.	σ(300 V) Ω	temp. °C	D. P. °C	RH %	∂	
1	14	$1.1 \cdot 10^{10}$	23.5	10	43	1.47	*
1	15	$1.0 \cdot 10^{12}$	21.5	8	42	5.00	
1	16	$4.5 \cdot 10^{11}$	22.5	9	43	3.84	*
1	17	$4.3 \cdot 10^{11}$	22.6	9	43	3.63	*
1	20	$4.6 \cdot 10^{11}$	23.2	9	40	4.29	
1	21	$1.3 \cdot 10^{11}$	20.5	7/8	43	5.35	*
1	22	$1.8 \cdot 10^{10}$	21.2	9	46	1.45	**
1	54	$1.0 \cdot 10^{12}$	21.0	8	44	2.39	*
1	55	$1.7 \cdot 10^{12}$	22.1	10	47	4.17	
2	1	$2.1 \cdot 10^{09}$	23.8	9	39	1.06	
2	3	$1.5 \cdot 10^{09}$	22.2	8	40	1.03	
2	8	$8.4 \cdot 10^{10}$	24.0	1	22	1.60	
2	9	$3.9 \cdot 10^{11}$	21.1	-2	22	1.45	
2	24	$6.1 \cdot 10^{11}$	22.1	0/1	24	1.74	
2	25	$1.5 \cdot 10^{09}$	18.9	6	41	1.16	
2	26	$1.2 \cdot 10^{09}$	20.4	7	42	1.06	*
2	27	$1.2 \cdot 10^{09}$	20.9	8	43	1.06	*
2	28	$7.8 \cdot 10^{08}$	21.8	9	44	1.10	**
2	29	$7.1 \cdot 10^{08}$	22.0	9	44	1.09	**
2	52	$4.3 \cdot 10^{13}$	20.2	-5	18	----	
2	53	$9.3 \cdot 10^{13}$			≈14	----	
2A	5	$8.6 \cdot 10^{10}$	23.9	1	22	1.60	
2A	12	$3.4 \cdot 10^{11}$	21.5	-2	21	1.39	
3	41	$5.5 \cdot 10^{10}$	20.0	7	43	1.10	*
3	42	$4.8 \cdot 10^{10}$	20.1	7	43	1.10	*
3	43	$2.2 \cdot 10^{10}$	19.5	7	44	1.10	*
3	44	$1.8 \cdot 10^{10}$	20.1	7	43	0.92	*
3	42A	$1.7 \cdot 10^{10}$	20.5	7	42	0.99	
3	45	$2.0 \cdot 10^{10}$	21.0	8	43	0.95	*
3	46	$1.4 \cdot 10^{13}$	20.5	-3/-2	22	----	
3	56	$2.3 \cdot 10^{10}$	22.8	10	44	0.91	*
4	47	$2.8 \cdot 10^{14}$	20.6	-3	21	----	
4	48	$5.1 \cdot 10^{10}$	20.4	8	45	1.09	*
4	49	$5.6 \cdot 10^{10}$	20.1	8	46	1.06	
5	31	$1.2 \cdot 10^{10}$	20.2	8	46	2.27	**
5	34	$1.7 \cdot 10^{10}$	21.5	9	45	1.65	*
5	36	$1.8 \cdot 10^{10}$	21.5	9	45	1.67	*
5	37	$4.6 \cdot 10^{12}$	20.2	6	39	2.36	
5	38	$3.9 \cdot 10^{11}$	20.0	7	43	1.52	**
5	39	$1.3 \cdot 10^{12}$	18.6	6	44	2.50	
5	40	$1.9 \cdot 10^{12}$	18.9	6	43	2.06	
6	50	$8.7 \cdot 10^{11}$	21.1	8/9	45	2.60	*
6	51	$1.3 \cdot 10^{12}$	20.0	8	46	1.69	

* measurement used for table 2.

** condensed water on surface.

table 5: Complete set of measurements.

Appendix B

POTCALC/13I
DATE & TIME PRINTED: THURSDAY, APRIL 16, 1987 @ 13:43:24.

```
  100     BEGIN
  200     $ INCLUDE "PLOTTER/ALGOL/DECLARATION ON APPL"
  300     $ INCLUDE "PLOTTER/ALGOL/NEWOBJECT ON APPL"
  400     $ INCLUDE "PLOTTER/ALGOL/CONTOUR1 ON APPL"
  500     $ INCLUDE "PLOTTER/ALGOL/POLYGON ON APPL"
  600     $ INCLUDE "PLOTTER/ALGOL/STRAIGHTLINEPIECE ON APPL"
  700     $ INCLUDE "PLOTTER/ALGOL/MAPANDDRAWOBJECT1 ON APPL"
  800     $ INCLUDE "PLOTTER/ALGOL/CLEAROBJECT ON APPL"
  900     $ INCLUDE "PLOTTER/ALGOL/AXISCOMPLETE ON APPL"
 1000     $ INCLUDE "PLOTTER/ALGOL/COMMENTTEXT ON APPL"
 1100     $ INCLUDE "PLOTTER/ALGOL/COMMENTNNUMBER ON APPL"
 1200     $ INCLUDE "PLOTTER/ALGOL/DRAWOBJECT ON APPL"
 1300     $ INCLUDE "PLOTTER/ALGOL/DISPOSEOBJECT ON APPL"
 1400     $ INCLUDE "NUMLIB/ALGOL/DECLARATION ON APPL"
 1500     $ INCLUDE "NUMLIB/ALGOL/DEC ON APPL"
 1600     $ INCLUDE "NUMLIB/ALGOL/DECINV ON APPL"
 1700     $ INCLUDE "NUMLIB/ALGOL/AMAALV ON APPL"
 1800       FILE IN(KIND=REMOTE), OUT(KIND=REMOTE);
 1900     % THIS VERSION OF THE POTCALC PROGRAM IS MADE FOR INTERACTIVE USE
 2000     % THE FILES THAT ARE USED ARE: IN(REMOTE), OUT(REMOTE),
 2100     % PR(PRINTER), PLOT(PREVIEWER)
 2200
 2300     %-----***** START INPUT
 2400
 2500       INTEGER N;
 2600       WRITE(OUT,<"NUMBER OF WIRES (HV-LINES + GROUND WIRES)">);
 2700       READ(IN,/,N);
 2800
 2900       BEGIN
 3000         REAL ARRAY L[1:N,1:3], VLR,VLI,QR,QI[1:N], P[1:N,1:N];
 3100         REAL F1,F2,EPS, VM;
 3200         INTEGER I,J,Q;
 3300         STRING PHASE;
 3400         WRITE(OUT,<"CHOOSE: PHASE (R,S,T,O) INPUT = 1, VOLTAGE",
 3500                    " (COMPLEX) INPUT = 2">);
 3600         READ(IN,/,Q);
 3700         IF Q=1 THEN
 3800           BEGIN
 3900             REAL PHV;
 4000             WRITE(OUT,<"GIVE PHASE VOLTAGE (KV)">);
 4100             READ(IN,/,PHV);
 4200             WRITE(OUT,<"SPECIFY EACH WIRE: DIAM.(M), X(M), Y(M), PHASE",
 4300                        "(R,S,T,O)">);
 4400             FOR I:=1 STEP 1 UNTIL N DO
 4500               BEGIN
 4600                 READ(IN,/,L[I,1],L[I,2],L[I,3],PHASE);
 4700                 IF PHASE="R" THEN BEGIN VLR[I]:=PHV; VLI[I]:=0; END;
 4800                 IF PHASE="S" THEN BEGIN VLR[I]:=-1*PHV/2;
 4900                                         VLI[I]:=-1*PHV*SQRT(3)/2; END;
 5000                 IF PHASE="T" THEN BEGIN VLR[I]:=-1*PHV/2;
 5100                                         VLI[I]:=PHV*SQRT(3)/2; END;
 5200                 IF PHASE="O" THEN VLI[I]:=VLR[I]:=0;
 5300               END;
 5400           END;
 5500         IF Q=2 THEN
 5600           BEGIN
 5700             WRITE(OUT,<"SPECIFY EACH WIRE: DIAM.(M), X(M), Y(M),"
 5800                        " VR(KV), VI(KV)">);
```

```
5900            FOR I:=1 STEP 1 UNTIL N DO READ(IN,/,L[I,1],L[I,2],L[I,3],
6000                                                VLR[I],VLI[I]);
6100          END;
6200
6300      %-----***** END INPUT / START CALCULATIONS
6400
6500          EPS:=1000*8.8543@-12;       % BECAUSE: V(KV) AND Q(C)
6600          F1:=1/(4*EPS*ARCSIN(1));
6700          F2:=F1/2;
6800          FOR I:=1 STEP 1 UNTIL N DO
6900            BEGIN
7000              FOR J:=1 STEP 1 UNTIL N DO
7100                IF I=J THEN P[I,I]:=F1*LN(4*L[I,3]/L[I,1])
7200                  ELSE
7300                    P[I,J]:=-F2*LN(((L[I,2]-L[J,2])**2+(L[I,3]-L[J,3])**2)/
7400                                   ((L[I,2]-L[J,2])**2+(L[I,3]+L[J,3])**2));
7500            END;
7600
7700          BEGIN
7800          % DETERMINING THE LINE-CHARGES
7900          %
8000            INTEGER ARRAY PP[1:N]; REAL CA; BOOLEAN SINGULAR;
8100            DEC(1,N,P,PP,SINGULAR,CA);
8200            IF SINGULAR THEN WRITE(OUT,<"SINGULAR=TRUE">);
8300            WRITE(OUT,<"CA=",E8.1>,CA);
8400            DECINV(1,N,P,PP);
8500            AMAALV(1,N,P,VLR,QR);
8600            AMAALV(1,N,P,VLI,QI);
8700          END;
8800
8900          BEGIN
9000          % DETERMINING THE MAXIMUM VOLTAGE VM
9100          %
9200            REAL V1;
9300            I:=1; VM:=0;
9400            WHILE I<=N DO
9500              BEGIN
9600                V1:=SQRT(VLR[I]**2+VLI[I]**2);
9700                IF V1>VM THEN VM:=V1;
9800                I:=I+1;
9900              END;
10000         END;
10100         WRITE(OUT,<"QR[1:N] AND QI[1:N] ARE KNOWN NOW">);
10200
10300     %-----***** END CALCULATIONS / START OUTPUT
10400
10500         BEGIN
10600         % OUTPUT PROGRAMM:
10700         %   OUTPUT 1: COMPLEX VOLTAGE IN ANY POINT X,Y IS GIVEN
10800         %             ON THE TERMINAL
10900         %   OUTPUT 2: COMPLETE SET OF CAPACITANCES, LINE-GROUND
11000         %             AND LINE-LINE, IS GIVEN ON PAPER
11100         %   OUTPUT 3: FIELD STRENGHT CALCULATION IN POINT X,Y
11200         %   OUTPUT 4: AN ARRAY IS FILLED WITH VOLTAGES IN AREA
11300         %             -XMAX:XMAX,0:YMAX AND PRINTED
11400         %   OUTPUT 5: EQUIPOTENTIAL LINES ARE DRAWN IN AREA
11500         %             -XMAX:XMAX,0:YMAX BY ELECTROSTATIC PLOTTER
11600         %
11700           INTEGER OUTPUT, Q;
11800           REAL X,Y, VRXY, VIXY, VXY;
11900           STRING TONA;
12000
```

```
12100           PROCEDURE VRI(PX,PY,PVRXY,PVIXY);
12200            % THIS PROCEDURE CALCULATES THE REAL AND IMAGINAR
12300            % PART OF THE VOLTAGE (PVRXY AND PVIXY)  IN A GIVEN POINT PX,PY
12400            % WHEN ALL QR[1:N] AND QI[1:N] ARE KNOWN.
12500            % IF PX,PY IS INSIDE A WIRE, THEN THE GIVEN WIRE-VOLTAGES
12600            % ARE COPIED IN PVRXY AND PVIXY.
12700             VALUE PX, PY; REAL PX, PY,PVRXY,PVIXY;
12800             BEGIN
12900               INTEGER I,J;
13000               REAL K; BOOLEAN F;
13100               J:=1; F:=FALSE;
13200               WHILE (NOT F AND J<=N) DO
13300                 BEGIN
13400                   IF ((PX-L[J,2])**2)+((PY-L[J,3])**2)<=(L[J,1]/2)**2
13500                     THEN
13600                       BEGIN
13700                         PVRXY:=VLR[J]; PVIXY:=VLI[J];
13800                         F:=TRUE
13900                       END;
14000                   J:=J+1;
14100                 END;
14200               IF NOT F THEN
14300                 BEGIN
14400                   PVRXY:=0;
14500                   PVIXY:=0;
14600                   FOR I:=1 STEP 1 UNTIL N DO
14700                     BEGIN
14800                       REAL K;
14900                       K:=-LN(((L[I,2]-PX)**2+(L[I,3]-PY)**2)/
15000                              ((L[I,2]-PX)**2+(L[I,3]+PY)**2));
15100                       PVRXY:=PVRXY+QR[I]*F2*K;
15200                       PVIXY:=PVIXY+QI[I]*F2*K;
15300                     END;
15400                 END;
15500           END;
15600
15700           WRITE(OUT,<"GIVE NAME OF TOWER">);
15800           READ(IN,/,TONA);
15900
16000           WRITE(OUT,<"WHAT OUTPUT DO YOU WANT (1-5)?">);
16100           WRITE(OUT,<"1: COMPLEX VOLTAGE IN X,Y (TERMINAL)">);
16200           WRITE(OUT,<"2: CAPACITANCES (PRINTER)">);
16300           WRITE(OUT,<"3: FIELD STRENGTH IN POINT X,Y (TERMINAL)">);
16400           WRITE(OUT,<"4: ARRAY OF VOLTAGES (PRINTER)">);
16500           WRITE(OUT,<"5: EQUIPOTENTIAL LINES (PREVIEWER)">);
16600           READ(IN,/,OUTPUT);
16700
16800           WHILE (OUTPUT<6) AND (OUTPUT>0) DO
16900             BEGIN
17000
17100               IF OUTPUT=1 THEN   % OUTPUT 1111111111111111111111111111111
17200                 BEGIN
17300                   INTEGER A;
17400                   WRITE(OUT,<"TOWER = ",A12>,TONA);
17500                   A:=11;
17600                   WHILE A=11 DO
17700                     BEGIN
17800                       WRITE(OUT,<"GIVE: X(M),Y(M)">);
17900                       READ(IN,/,X,Y);
18000                       VRI(X,Y,VRXY,VIXY);
18100                       VXY:=SQRT(VRXY**2+VIXY**2);
18200                       WRITE(OUT,<"VR(X,Y)=",E10.3," KV">,VRXY);
```

```
18300                   WRITE(OUT,<"VI(X,Y)=",E10.3," KV">,VIXY);
18400                   WRITE(OUT,<"V(X,Y) =",E10.3," KV">,VXY);
18500                   WRITE(OUT,</,"MORE POINTS? YES=11, NO=5">);
18600                   READ(IN,/,A);
18700                 END;
18800               END;
18900
19000             IF OUTPUT=2 THEN   % OUTPUT 22222222222222222222222222222
19100               BEGIN
19200                 FILE PR(KIND=PRINTER);
19300                 REAL ARRAY C[1:N,1:N];
19400                 INTEGER II;
19500                 FOR I:=1 STEP 1 UNTIL N DO
19600                   FOR J:=1 STEP 1 UNTIL N DO
19700                     BEGIN
19800                       IF I=J THEN
19900                         BEGIN
20000                           C[I,I]:=0;
20100                           FOR II:=1 STEP 1 UNTIL N DO
20200                                   C[I,I]:=C[I,I]+P[I,II]*1@-3;
20300                         END
20400                        ELSE C[I,J]:=-P[I,J]*1@-3;
20500                     END;
20600                 WRITE(PR,<"TOWER = ",A20>,TONA);
20700                 WRITE(PR,<"WIRES:">);
20800                 WRITE(PR,<X2,"X(M)",X5,"Y(M)",X4,"DIAM(M)",X9,
20900                          "VOLTAGE">);
21000                 FOR I:=1 STEP 1 UNTIL N DO
21100                   WRITE(PR,<F6.2,F9.2,F11.5,F11.3," +J(",F8.3,")KV">,
21200                         L[I,2],L[I,3],L[I,1],VLR[I],VLI[I]);
21300                 WRITE(PR,</,"CAPACITANCES OF ",A20," ARE (F/M):",/>,
21400                       TONA);
21500                 FOR I:=1 STEP 1 UNTIL N DO
21600                  IF N>9 THEN WRITE(PR,*/,N,C[I,*])
21700                         ELSE WRITE(PR,<*E14.5>,N,C[I,*]);
21800                 WRITE(OUT,<"USE: ^U$SERVICE/BACKUP ON APPL^ TO PRINT">);
21900               END;
22000
22100
22200             IF OUTPUT=3 THEN   % OUTPUT 33333333333333333333333333333
22300               BEGIN
22400                 INTEGER CALCTYPE, CN;
22500                 REAL ARRAY E[1:2];
22600
22700                 PROCEDURE EFIELD(X,Y,EA);
22800                     %
22900                     % THIS PROCEDURE CALLCULATES THE ABSOLUTE VALUES
23000                     % OF THE COMPLEX EL. FIELD STRENGTH IN (X,Y);
23100                     % DELIVERED IN EX AND EY
23200                  VALUE X,Y; REAL X,Y; REAL ARRAY EA[*];
23300                    BEGIN
23400                     COMPLEX ARRAY E[1:2];
23500                     E[1]:=E[2]:=COMPLEX(0,0);
23600                     FOR I:=1 STEP 1 UNTIL N DO
23700                       BEGIN
23800                         COMPLEX F;
23900                         F:=250*COMPLEX(QR[I],QI[I])/(EPS*ARCSIN(1));
24000                         E[1]:=E[1]+F*(X-L[I,2])/(((X-L[I,2])**2)+
24100                                                  ((Y-L[I,3])**2))
24200                                   -F*(X-L[I,2])/(((X-L[I,2])**2)+
24300                                                  ((Y+L[I,3])**2));
24400                         E[2]:=E[2]+F*(Y-L[I,3])/(((X-L[I,2])**2)+
```

```
24500                                                ((Y-L[I,3])**2))
24600                                -F*(Y+L[I,3])/(((X-L[I,2])**2)+
24700                                                ((Y+L[I,3])**2));
24800                       END;
24900                    EA[1]:=CABS(E[1]);
25000                    EA[2]:=CABS(E[2]);
25100                END;
25200
25300               WRITE(OUT,<"CHOOSE: FIELD STRENGHT CALCULATION ",
25400                         "IN POINT = 1">);
25500               WRITE (OUT,<X8,"MAX. FIELD ON CONDUCTOR = 2">);
25600               READ (IN,/,CALCTYPE);
25700               IF CALCTYPE=1 THEN
25800                 BEGIN
25900                   WRITE(OUT,<"GIVE: X, Y">);
26000                   READ(IN,/,X,Y);
26100                   EFIELD(X,Y,E);
26200                   WRITE(OUT,<"EX=",E10.3," V/M">,E[1]);
26300                   WRITE(OUT,<"EY=",E10.3," V/M">,E[2]);
26400                   WRITE(OUT,<"/E/=",E10.3," V/M">,SQRT(E[1]**2+
26500                                                        E[2]**2));
26600                 END;
26700               IF CALCTYPE=2 THEN
26800                    %
26900                    % EMAX ON CONDUCTOR CN IS DETERMINED WITH THE
27000                    % METHOD OF THE GOLDEN CUT
27100                    %
27200                BEGIN
27300                 REAL A, B, T, T2, Z, ZA, F, FA, AN;
27400                 A:=1@-5; B:=360; T:=1.618; T2:=1.618**2;
27500                 Z:=A/T+B*(1-1/T);  ZA:=A/T2+B*(1-1/T2);
27600                 WRITE(OUT,<"GIVE INPUT SEQUENCE NUMBER OF CONDUCTOR">);
27700                 READ(IN,/,CN);
27800                 WHILE ABS((Z-ZA)/ZA)>1@-7 DO
27900                  BEGIN
28000                   AN:=ARCSIN(1)*4*Z/360;
28100                   X:=L[CN,2]+L[CN,1]*COS(AN)/2;
28200                   Y:=L[CN,3]+L[CN,1]*SIN(AN)/2;
28300                   EFIELD(X,Y,E);
28400                   F:=SQRT(E[1]**2+E[2]**2);
28500                   AN:=ARCSIN(1)*4*ZA/360;
28600                   X:=L[CN,2]+L[CN,1]*COS(AN)/2;
28700                   Y:=L[CN,3]+L[CN,1]*SIN(AN)/2;
28800                   EFIELD(X,Y,E);
28900                   FA:=SQRT(E[1]**2+E[2]**2);
29000                   IF FA<F THEN
29100                            BEGIN
29200                             B:=ZA; ZA:=Z;
29300                             Z:=A/T+B*(1-1/T);
29400                            END
29500                           ELSE
29600                            BEGIN
29700                             A:=Z; Z:=ZA;
29800                             ZA:=A/T2+B*(1-1/T2);
29900                            END;
30000                  END;
30100                 AN:=ARCSIN(1)*4*Z/360;
30200                 X:=L[CN,2]+L[CN,1]*COS(AN)/2;
30300                 Y:=L[CN,3]+L[CN,1]*SIN(AN)/2;
30400                 EFIELD(X,Y,E);
30500                 WRITE(OUT,<"EMAX ON CONDUCTOR",I3," IS",E12.4," V/M">,
30600                       CN,SQRT(E[1]**2+E[2]**2));
```

```
30700                   WRITE(OUT,<"IN: (X,Y)= (",E10.3,",",E10.3,
30800                         ") (M,M)">,X,Y);
30900                   WRITE(OUT,<"AND ALPHA =",F7.1," DEG">,Z);
31000                  END;
31100                END;
31200
31300              IF OUTPUT=4 THEN   % OUTPUT 44444444444444444444444444444444
31400                BEGIN
31500                  REAL XM, YM, SF;
31600                  INTEGER M;
31700                  WRITE(OUT,<"GIVE: XMAX(M),YMAX(M)">);
31800                  READ(IN,/,XM,YM);
31900                  SF:=2*XM/32; M:=YM DIV SF;
32000                  BEGIN
32100                    FILE PR(KIND=PRINTER);
32200                    REAL X,Y; REAL ARRAY V[-15:15];
32300                    WRITE(PR,<"TOWER = ",A12,/>,TONA);
32400                    WRITE(PR,<"Y(M)",X4,"V(X,Y)(KV)">);
32500                    FOR I:=1 STEP 1 UNTIL M DO
32600                      BEGIN
32700                        Y:=(M+1-I)*SF;
32800                        FOR J:=-15 STEP 1 UNTIL 15 DO
32900                          BEGIN
33000                            X:=J*SF;
33100                            VRI(X,Y,VRXY,VIXY);
33200                            V[J]:=SQRT(VRXY**2+VIXY**2);
33300                          END;
33400                        WRITE(PR,<I4,X2,*I4>,Y,31,V[*]);
33500                      END;
33600                    FOR J:=-15 STEP 1 UNTIL 15 DO V[J]:=J*SF;
33700                    WRITE(PR,</,X6,*I4>,31,V[*]);
33800                    WRITE(PR,<X126,"X(M)">);
33900                    WRITE(PR,</,"WIRES:">);
34000                    WRITE(PR,<X2,"X(M)",X5,"Y(M)",X4,"DIAM(M)",X9,
34100                              "VOLTAGE">);
34200                    FOR I:=1 STEP 1 UNTIL N DO
34300                      WRITE(PR,<F6.2,F9.2,F11.5,F11.3," +J(",F8.3,")KV">,
34400                            L[I,2],L[I,3],L[I,1],VLR[I],VLI[I]);
34500                  END;
34600                  WRITE(OUT,<"USE: 'U$SERVICE/BACKUP' TO PRINT">);
34700                END;
34800
34900              IF OUTPUT=5 THEN   % OUTPUT 55555555555555555555555555555
35000                BEGIN
35100                  REAL XM, YM, SF; INTEGER M;
35200                  WRITE(OUT,<"GIVE: XMAX(M),YMAX(M)">);
35300                  READ(IN,/,XM,YM);
35400                  SF:=2*XM/81; M:=YM DIV SF;
35500                  BEGIN
35600                    FILE PLOT(KIND=PREVIEWER);
35700                    INTEGER OBJ,I,J,Q1,NPARTS,PART;
35800                    REAL ARRAY XA[0:80], YA[0:M], VA[0:80,0:M],
35900                              XISO,YISO[1:85,1:900], XB,YB[0:80,0:M];
36000                    INTEGER ARRAY NPOINTS,PKIND[1:85];
36100                     % DECLARATION OF THESE ARRAYS IN THIS WAY
36200                     % FIXES A MAXIMUM NUMBER OF CONTOURPARTS (FOR ONE
36300                     % VALUE OF FO) OF 85 AND A MAXIMUM NUMBER OF POINTS
36400                     % FOR ONE CONTOUR OF 900.
36500                    REAL VX,VY,VV,FO;
36600                    STRING STR1, STR2, STR3;
36700                    FOR I:=0 STEP 1 UNTIL 80 DO
36800                        XA[I]:=(-40+I)*SF;
```

```
36900                   FOR I:=0 STEP 1 UNTIL M DO
37000                       YA[I]:=I*SF;
37100                   FOR I:=0 STEP 1 UNTIL 80 DO
37200                     FOR J:=0 STEP 1 UNTIL M DO
37300                       BEGIN
37400                         VRI(XA[I],YA[J],VRXY,VIXY);
37500                         VA[I,J]:=SQRT(VRXY**2+VIXY**2)/VM;
37600                       END;
37700                   Q1:=11;
37800                   NEWOBJECT(OBJ);
37900                   FOR I:=0 STEP 1 UNTIL 80 DO
38000                     BEGIN
38100                       FOR J:=0 STEP 1 UNTIL M DO
38200                         BEGIN
38300                           XB[I,J]:=XA[I];
38400                           YB[I,J]:=YA[J];
38500                         END;
38600                     END;
38700                   FOR FO:=0.001,.005,.01,.02,.05,.1,.15,
38800                           .2,.25,.3,.4,.6,.8,0.95 DO
38900                     BEGIN
39000                       CONTOUR1(FO,0,80,0,M,XB,YB,VA,1,NPARTS,NPOINTS,
39100                                PKIND,XISO,YISO);
39200                       FOR PART:=1 STEP 1 UNTIL NPARTS DO
39300                         BEGIN
39400                           POLYGON(OBJ,I,1,NPOINTS[PART],XISO[PART,I],
39500                                   YISO[PART,I],1);
39600                           IF PKIND[PART]=1 THEN
39700                              STRAIGHTLINEPIECE(OBJ,XISO[PART,
39800                                                NPOINTS[PART]],YISO[PART,
39900                                                NPOINTS[PART]],XISO[PART,
40000                                                1],YISO[PART,1],1);
40100                         END;
40200                     END;
40300                   MAPANDDRAWOBJECT1(PLOT,OBJ,2,2,8.5*YM/XM+2,19,
40400                                     -1*XM,0,XM,0,XM,YM,2,19,2,2,
40500                                     8.5*YM/XM+2,2);
40600                   CLEAROBJECT(OBJ);
40700                   AXISCOMPLETE(OBJ,2,2,2,19,20,1,XM,-1*XM,TRUE,
40800                                FALSE,.2,"X(M)");
40900                   AXISCOMPLETE(OBJ,2,2,8.5*YM/XM+2,2,20,0,0,YM,
41000                                FALSE,FALSE,.2,"HEIGHT Y(M)");
41100             STR2:="EQUIPOTENTIAL LINES FOR V= 0.1,0.5,1,2,5,10,15,";
41200             STR3:="20,25,30,40,60,80,95 % OF        KV(PH-GR)";
41300                   STR1:=STR2 CAT STR3;
41400                   COMMENTTEXT(OBJ,8.5*YM/XM+3,19,-90,.2,0,STR1);
41500                   COMMENTNNUMBER(OBJ,8.5*YM/XM+3,4.6,-90,.2,0,
41600                                  "F6.1",VM);
41700                   COMMENTTEXT(OBJ,8.5*YM/XM+3+(N+2)*.4,19,-90,.2,
41800                               0,"WIRES:");
41900                   STR2:="TOWER = ";
42000                   STR1:=STR2 CAT TONA;
42100                   COMMENTTEXT(OBJ,8.5*YM/XM+3+(N+3)*.4,19,-90,.2,
42200                               0,STR1);
42300                   FOR I:=1 STEP 1 UNTIL N DO
42400                     BEGIN
42500                       STR1:="V(      ,      )=       +J(       )KV";
42600                       STR2:=", DIAM.=       CM";
42700                       STR3:=STR1 CAT STR2;
42800                       COMMENTTEXT(OBJ,8.5*YM/XM+3+(N+2-I)*.4,19,-90,.2,
42900                                   0,STR3);
43000                       COMMENTNNUMBER(OBJ,8.5*YM/XM+3+(N+2-I)*.4,18.6,
```

```
43100                                   -90,.2,0,"F6.2",L[I,2]);
43200                         COMMENTNNUMBER(OBJ,8.5*YM/XM+3+(N+2-I)*.4,17.2,
43300                                   -90,.2,0,"F6.2",L[I,3]);
43400                         COMMENTNNUMBER(OBJ,8.5*YM/XM+3+(N+2-I)*.4,15.6,
43500                                   -90,.2,0,"F7.2",VLR[I]);
43600                         COMMENTNNUMBER(OBJ,8.5*YM/XM+3+(N+2-I)*.4,13.6,
43700                                   -90,.2,0,"F7.2",VLI[I]);
43800                         COMMENTNNUMBER(OBJ,8.5*YM/XM+3+(N+2-I)*.4,10.0,
43900                                   -90,.2,0,"F7.2",L[I,1]*100);
44000                       END;
44100                     DRAWOBJECT(PLOT,OBJ,0,0,8.5*YM/XM+4+(N+2)*.4,20);
44200                     DISPOSEOBJECT(OBJ);
44300                     WRITE(OUT,<"PLOT IS READY">);
44400                   END;
44500                 END;
44600
44700               WRITE(OUT,<"ANOTHER OUTPUT? (1,2,3,4,5), 0 = STOP ">);
44800               READ(IN,/,OUTPUT);
44900             END;
45000         END;
45100       END;
45200     END.
```